# Baryon Electromagnetic Transition Form Factors: Current Knowledge

Teresa Peña

In Collaboration with Gilberto Ramalho,
Gernot Eichmann, André Torcato, Ana Arriaga

TÉCNICO LISBOA

LIP

DF DEPARTAMENTO DE FÍSICA TÉCNICO LISBOA

DECN DEPARTAMENTO DE ENGENHARIA E CIÊNCIAS NUCLEARES TÉCNICO LISBOA

FCT Fundação para a Ciência e a Tecnologia

REPÚBLICA PORTUGUESA

✓ **CLAS collaboration at JLab**

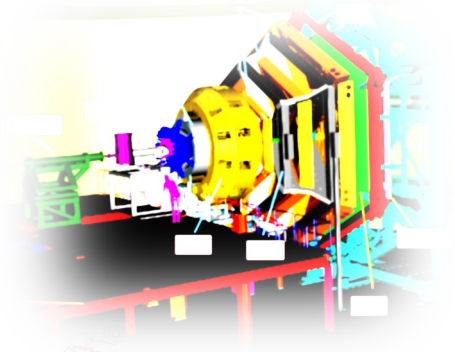

✓ **HADES collaboration at GSI**

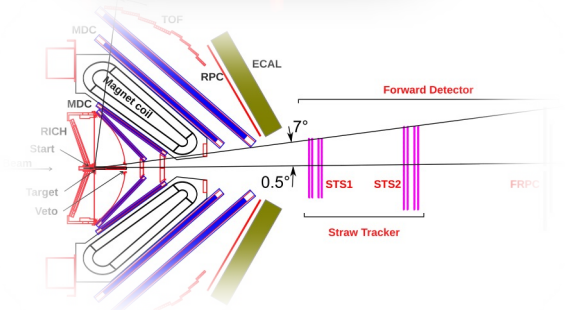


**Both enable studies of hadrons in the few GeV region;**
**probe electromagnetic couplings with**
**short-lived QCD systems.**

This talk:
Connects **TFF in different** kinematic regions
to obtain **Baryon-Photon coupling evolution** with 4 momentum transfer.

This evolution informs us on how structure properties of baryons
emerge from quarks and gluons.

# Electromagnetic Transition form factors (TFF)

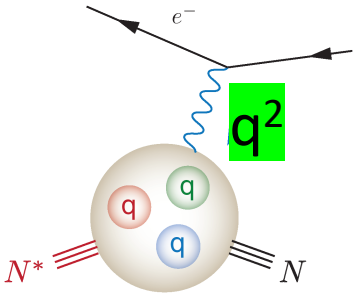


Baryon resonances **transition form factors**

CLAS: Aznauryan et al., Phys. Rev. C 80 (2009)

MAID: Drechsel, Kamalov, Tiator, EPJ A 34 (2009)

Gernot Eichmann and G. Ramalho
Phys. Rev. D 98, 093007 (2018)
Review: G. Ramalho and TP
Prog. Part. Nucl. Phys. 136 (2024) 104097

$q^2<0$

**Spacelike form factors:**

- Structure information:

qqq excitations vs. hybrid, charge and magnetization deformations not accessible from elastic FF alone

$q^2>0$

**Timelike form factors:**

- Particle production channels from scattering reactions
- Spectroscopic information: masses and widths

Role of SU(3) flavour-symmetry breaking, e.g. $\gamma^*\Sigma^+ \to \Sigma^{*+}$ versus $\gamma^* N \to \Delta$

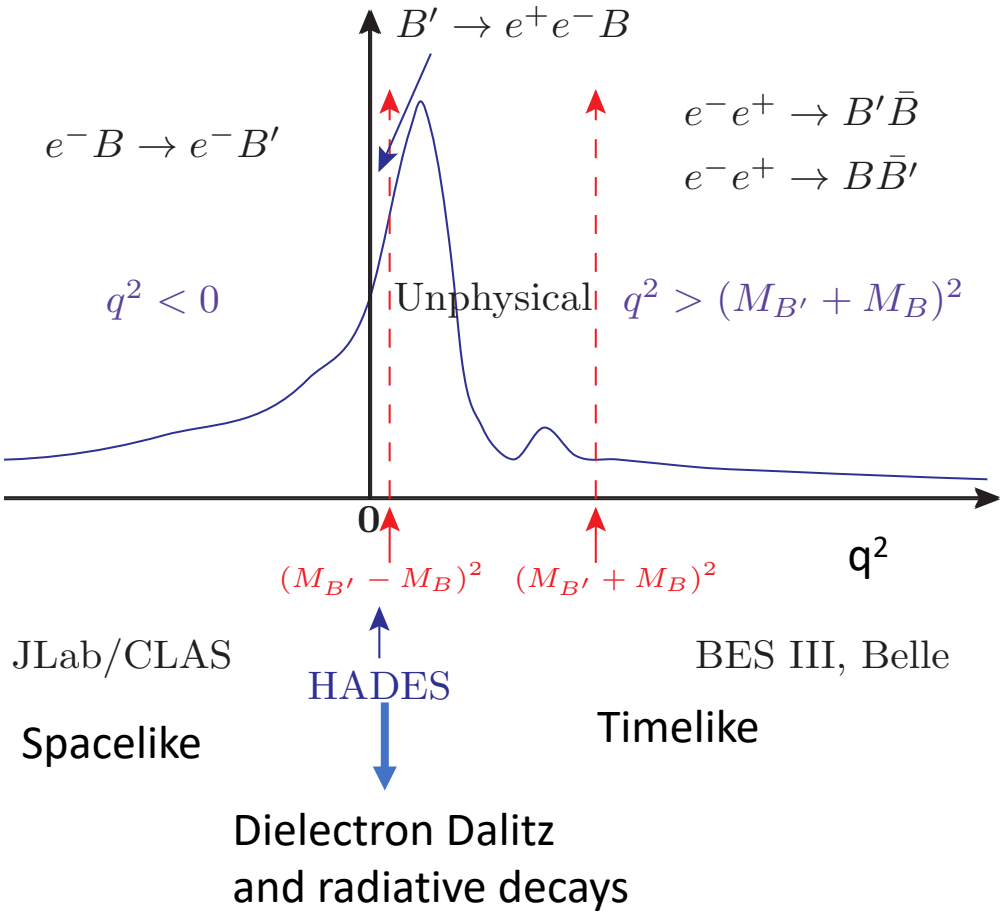
$B' \to e^+e^-B$
$e^-B \to e^-B'$
$e^-e^+ \to B'\bar{B}$
$e^-e^+ \to B\bar{B}'$
$q^2 < 0$
Unphysical
$q^2 > (M_{B'} + M_B)^2$
0
$(M_{B'} - M_B)^2$
$(M_{B'} + M_B)^2$
$q^2$
JLab/CLAS
HADES
BES III, Belle
Spacelike
Timelike
Dielectron Dalitz
and radiative decays

# Baryon resonances S=0 PDG

| $I$ | $S$ | $J^P = \frac{1}{2}^+$ | $\frac{3}{2}^+$ | $\frac{5}{2}^+$ | $\frac{1}{2}^-$ | $\frac{3}{2}^-$ | $\frac{5}{2}^-$ |
|---|---|---|---|---|---|---|---|
| $\frac{1}{2}$ | 0 | **N(940)**<br>**N(1440)**<br>$N(1710)$<br>$N(1880)$ | **N(1720)**<br>$N(1900)$ | **N(1680)**<br>$N(1860)$ | **N(1535)**<br>**N(1650)**<br>$N(1895)$ | **N(1520)**<br>$N(1700)$<br>$N(1875)$ | **N(1675)** |
| $\frac{3}{2}$ | 0 | **Δ(1910)** | **Δ(1232)**<br>$\Delta(1600)$<br>$\Delta(1920)$ | **Δ(1905)** | **Δ(1620)**<br>$\Delta(1900)$ | **Δ(1700)**<br>$\Delta(1940)$ | $\Delta(1930)$ |

Talk of Gilberto Ramalho extends this talk

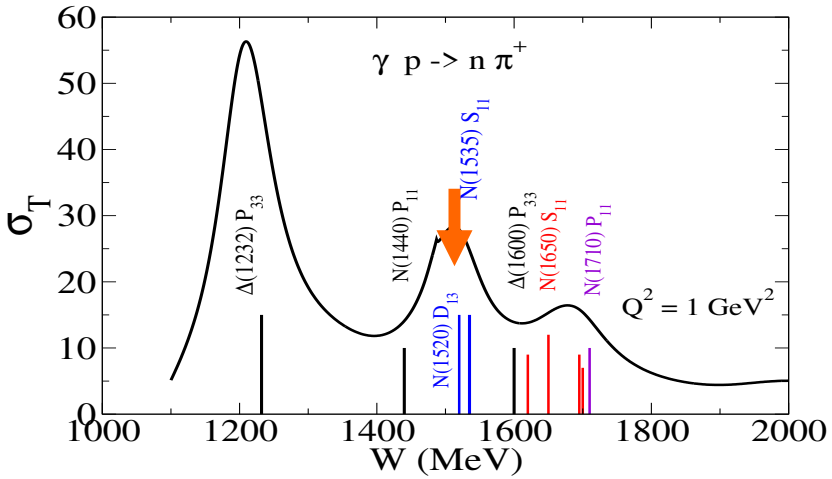

# Theoretical tools

Figs: courtesy of Gernot Eichmann

- **QCD Lagrangean in Space-Time grid & finite volume** → Lattice QCD

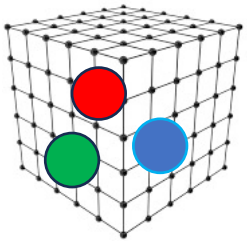

- **Analyticity** → Dispersion theory

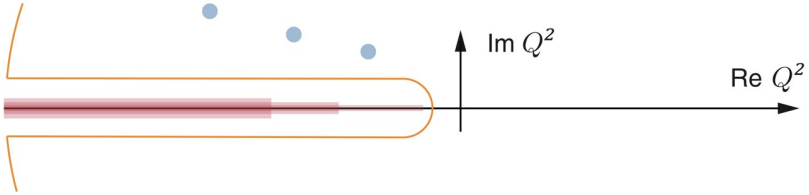


- **Functional methods in the continuum (Dynamics)** → Dyson-Schwinger Bethe-Salpeter eqs.

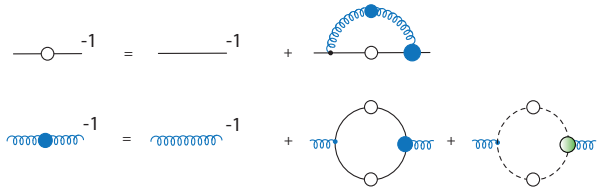


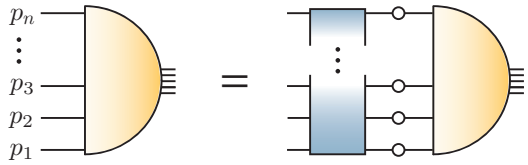


Guidance to the limits to the continuum and infinite volume
Identification of nonperturbative effects, as dynamical mass generation, internal clustering decomposition phenomena.

→ Effective Field Theory
→ Large $N_c$ limit
→ Quark models

Dyson–Schwinger methods deciphered the baryon spectrum (eg. C. Fischer talk): $N(1440)$, $N(1535)$ and N(1650) states correct relative position in the spectrum.

The combination of different diquark correlations in baryon structure explained it.

M.Y. Barabanov et al., Prog. Part. Nucl. Phys 116(2021) 103835

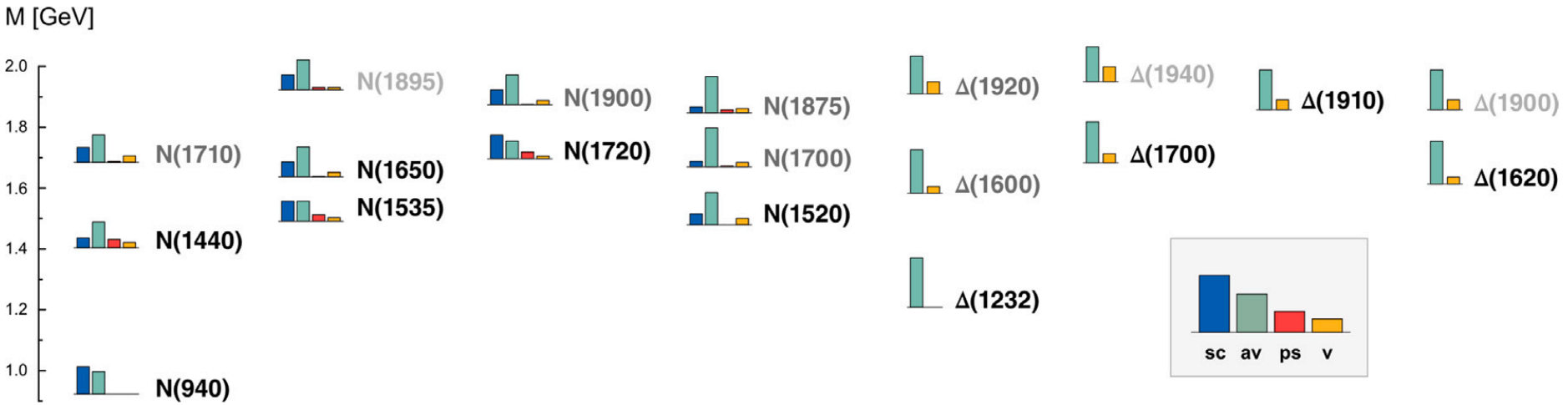


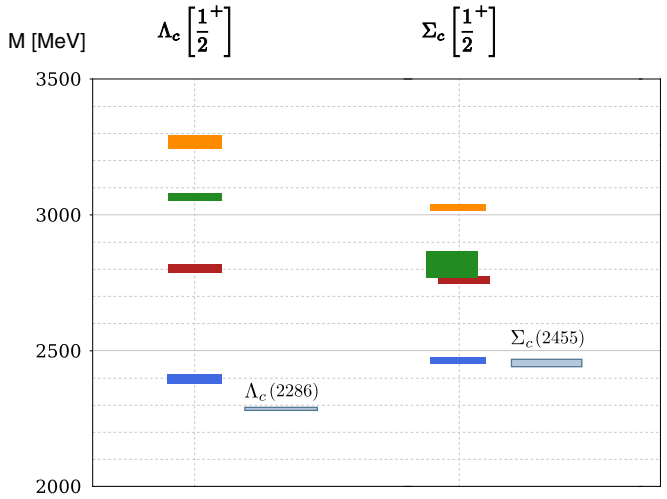



n-> u,d

## Recent calculation singly charmed Baryons

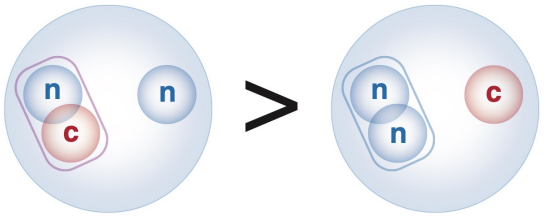


~60% ~40%

A. Torcato, A. Arriaga, G. Eichmann, M. T. P. Few Body Syst. 64 3, 45 (2023)

# E.M. matrix element

CST© 2008

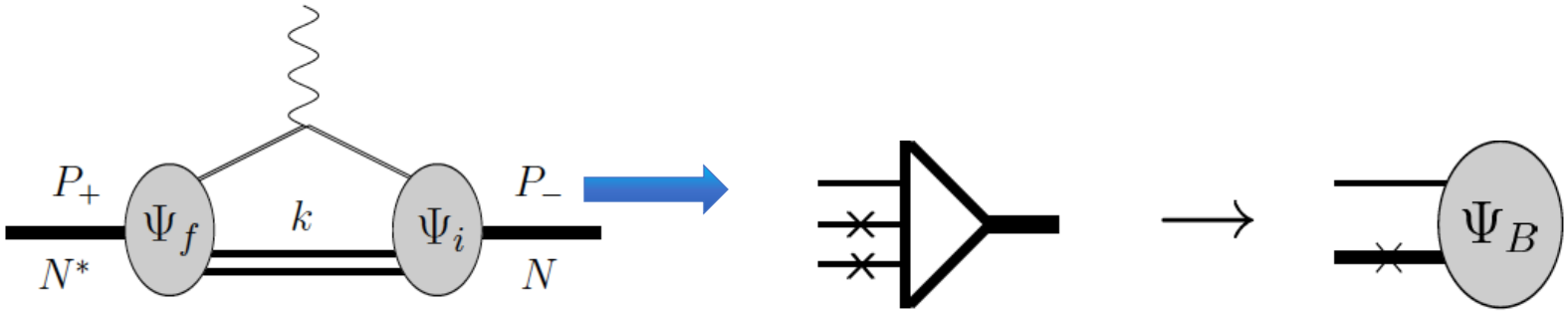


- **For the E.M. matrix element calculation,** the Baryon vertex is integrated over the spectator quarks variables.
(Covariant Spectator Model, **CST**)

- **A reduced quark - diquark Baryon** wave function is all that is needed;
it is phenomenologically constructed.

**G. Ramalho, TP, Franz Gross, Phys. Rev. D78, 114017 (2008)**

- ✓ The wf is symmetry based only; not dynamically generated
- ✓ The Diquark is not pointlike; it encloses structure

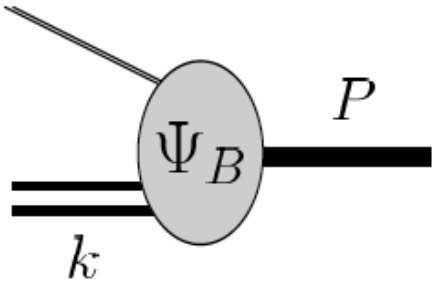


Eg. S-wave

- **Nucleon** "wavefunction"
  - A quark + **scalar**-diquark component
  - A quark+ **axial vector**-diquark component

- **Delta (1232)** "wavefunction"
  - Only quark + **axial vector**-diquark term contributes

Phenomenology comes into "radial" functions $\psi$

# Quark E.M. Current

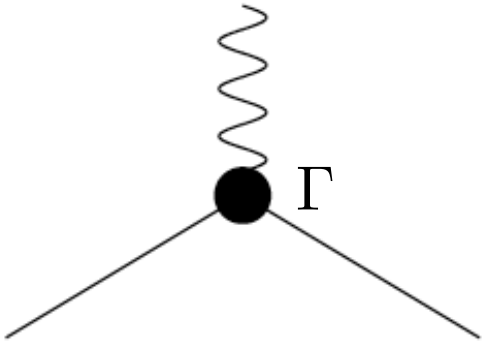


quark-antiquark

⊕ gluon dressing

Quark-photon vertex

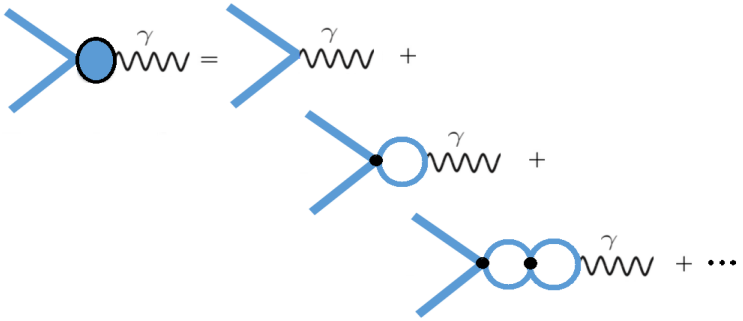

$$\Gamma_\mu(p,Q) = \gamma_\mu + \int \frac{d^4q}{(2\pi)^4} K(p,q,Q) S(q+\eta Q) \Gamma_\mu(q,Q) S(q-\eta Q)$$

Meson Spectrum is tied to this vertex

Constituent quarks (quark form factors)

$$j^\mu_I = \left[\frac{1}{6} f_{1+} + \frac{1}{2} f_{1-}\tau_3\right]\gamma^\mu + \left[\frac{1}{6} f_{2+} + \frac{1}{2} f_{2-}\tau_3\right]\frac{i\sigma^{\mu\nu}q_\nu}{2M_N}$$

To parametrize the e.m current we use **Vector Meson Dominance at the quark level,** with a

a truncation to the rho and omega poles of the full meson spectrum contribution to the quark-photon coupling.

**4** parameters

# VMD as link to LQCD

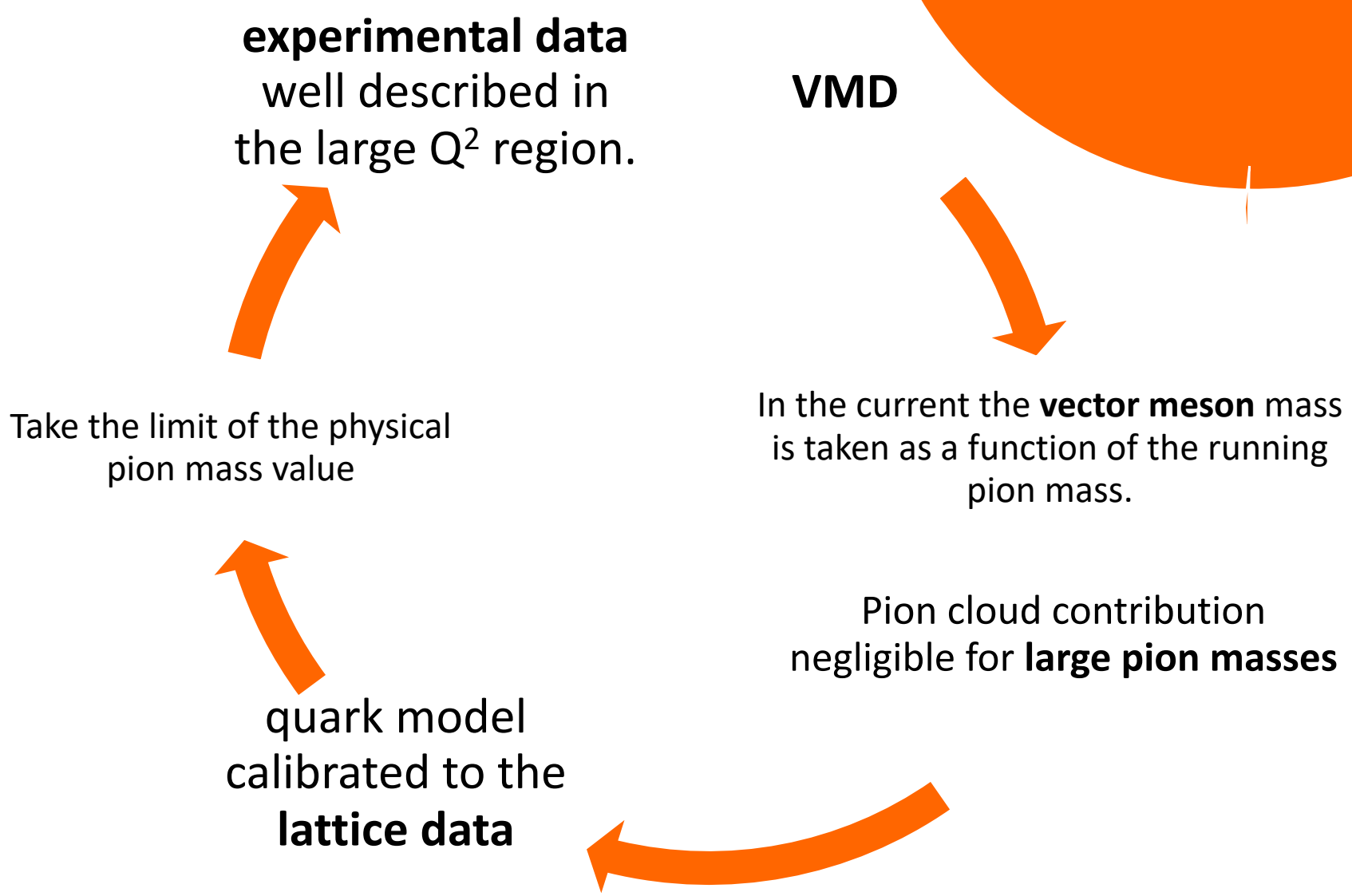

# Model independent feature

$$\gamma N \rightarrow \Delta$$

Talk of Gilberto Ramalho for details

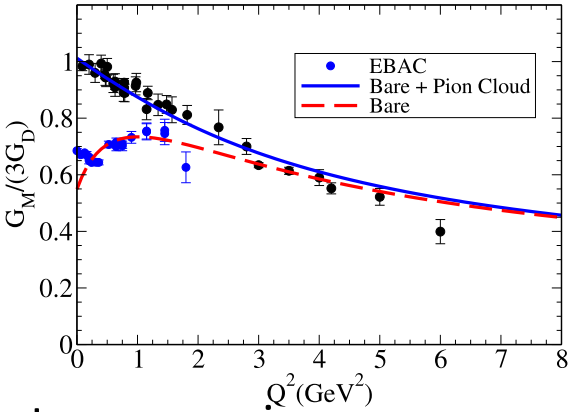


**Missing strength of** $G_M$ at the origin is an universal feature, even in dynamical quark calculations.

G. Eichmann, D. Nicmorus, Phys. Rev. D 85, 093004 (2012)

Eichmann et al., Prog. Part. Nucl. Phys. 91 (2016)

H. Sanchiz-Alepuz, R. Alkofer, C. Fischer, Phys. J A (2018) 54

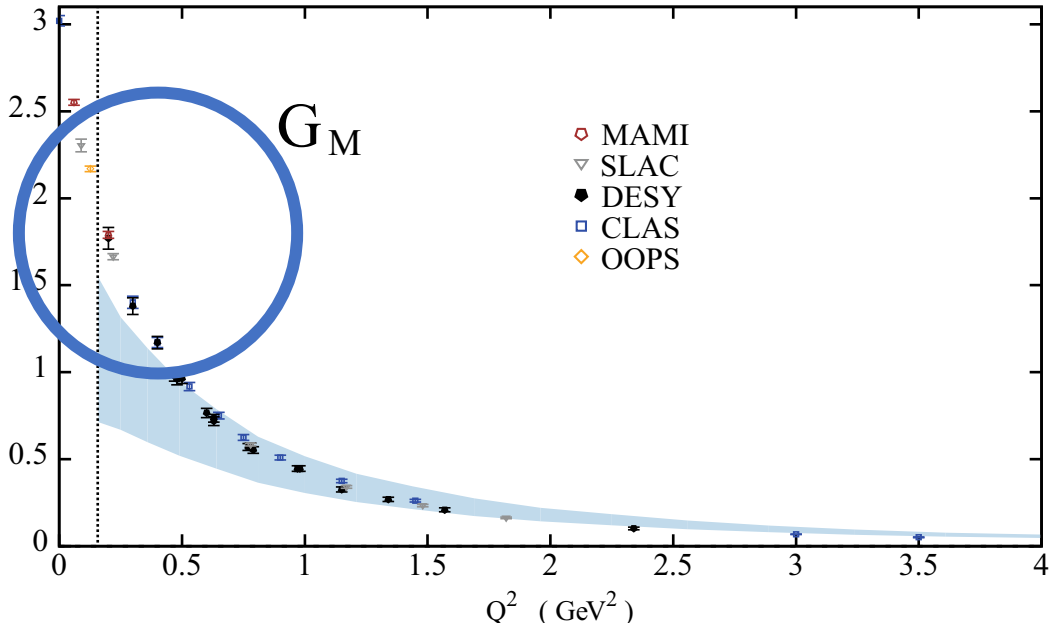


Effect of vicinity of the mass of the Delta to the pion-nucleon threshold.

Pion loop effects suppressed for high $Q^2$ $\frac{1}{Q^8}$

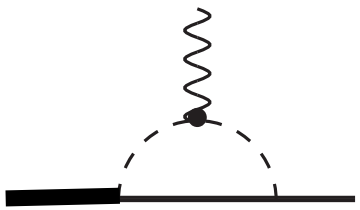

# E.M. Current and TFF below the photon point

$$\gamma N \rightarrow \Delta$$

$$\Gamma^{\beta\mu}(P,q) = \left[G_1 q^\beta \gamma^\mu + G_2 q^\beta P^\mu + G_3 q^\beta q^\mu - G_4 g^{\beta\mu}\right]\gamma_5$$

- Only 3 $G_i$ are independent.
  E.M. Current has to be conserved $\quad q^\mu \Gamma_{\beta\mu} = 0$

→ $G_M$, $G_E$, $G_C$ Scadron Jones popular choice.

- Only finite $G_i$ are physically acceptable.

From both requirements,
it follow an important constraint $\quad G_E(PT) = \frac{M_R - M}{2M_R} G_C(PT) \qquad Q_0^2 = -(M_R - M_N)^2 \;\; ; |\vec{Q}| = 0$

G.Ramalho Phys. Lett. B 759 (2016) 126 More in talk of Gilberto Ramalho

**Use** general nucleon-to-resonance transition
**form factors free of kinematic constraints to avoid missing physics constraints**

**Gernot Eichmann and Gilberto Ramalho**
**Phys. Rev. D 98, 093007 (2018)**

# $N \rightarrow N^*(1520)$ **TFFs**

$J^P=3/2^-$ I=1/2

60% decay $\pi$ N

30% decay to $\pi\Delta$

- Bare quark model gives good description in the high momentum transfer region.

- For low $Q^2$, failure of description hints to meson effects.

Consistent with Aznauryan and Burkert, PRC 85 055202 2012 and PDG

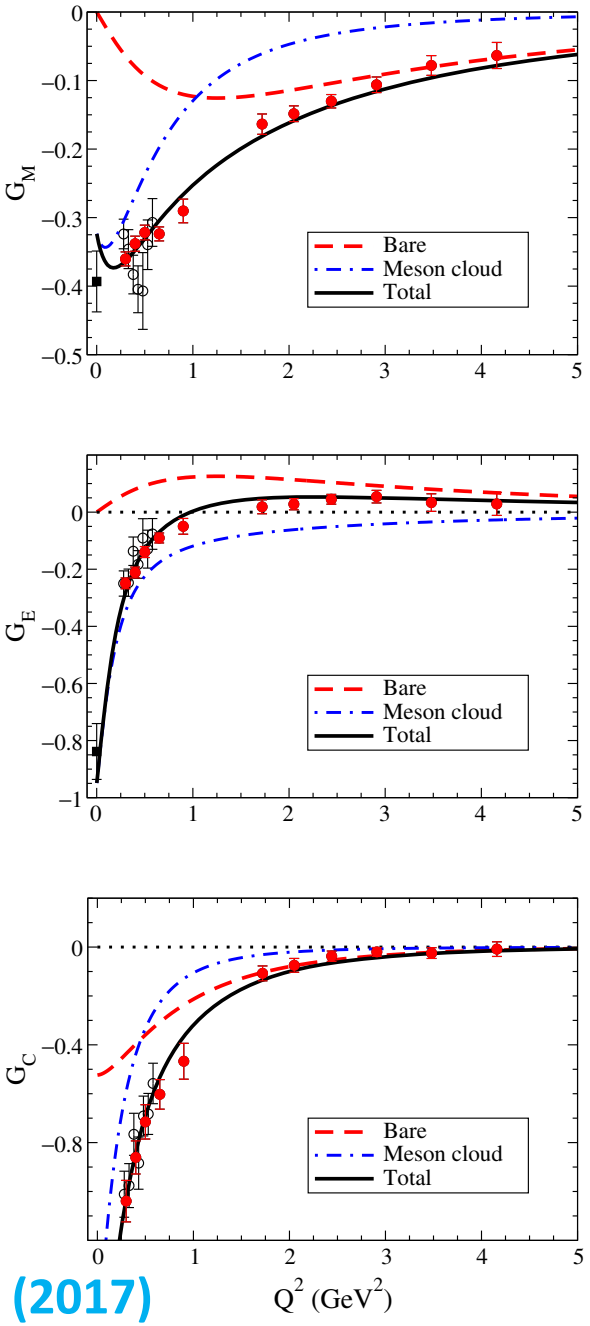


G. Ramalho, M. T. P. , PHYSICAL REVIEW D 95 014003 (2017)

# $N \rightarrow N^*(1520)$

PDG data at the photon point:

| | $A_{1/2}$ | $A_{3/2}$ | $\lvert A\rvert^2$ |
|---|---|---|---|
| $p$ | $-0.025 \pm 0.005$ | $0.140 \pm 0.005$ | $20.2 \pm 1.4$ |
| $n$ | $-0.050 \pm 0.005$ | $-0.120 \pm 0.005$ | $15.7 \pm 1.3$ |

$$A^V_{3/2} \approx 0.13 \; ; A^S_{3/2} \approx 0.01 \, (GeV^{-1/2})$$

Dominance of iso-vector channel concurs
to the interpretation of low $Q^2$ effects as “pion cloud effects”

# $N \to N^*(1535)$ TFFs

$J^P=1/2^-$ I=1/2
~50% decay to $\pi$N
~50% decay to $\eta$N

$$J^\mu = \bar{u}_R \left[ F_1^* \left( \gamma^\mu - \frac{\not{q} q^\mu}{q^2} \right) + F_2^* \frac{i\sigma^{\mu\nu} q_\nu}{M_N + M_R} \right] \gamma_5 u_N$$

- Again good agreement of bare quark core with data in the large $Q^2$ region.
- It dominates $F_1^*$ for large $Q^2$
- Meson effects in $F_2^*$ extend to high $Q^2$ region.

$$A^V_{1/2}(0) = 0.090 \pm 0.013 \text{ GeV}^{-1/2}$$
$$A^S_{1/2}(0) = 0.015 \pm 0.013 \text{ GeV}^{-1/2}$$

Effect from the $\eta$N together with $\pi$N channel

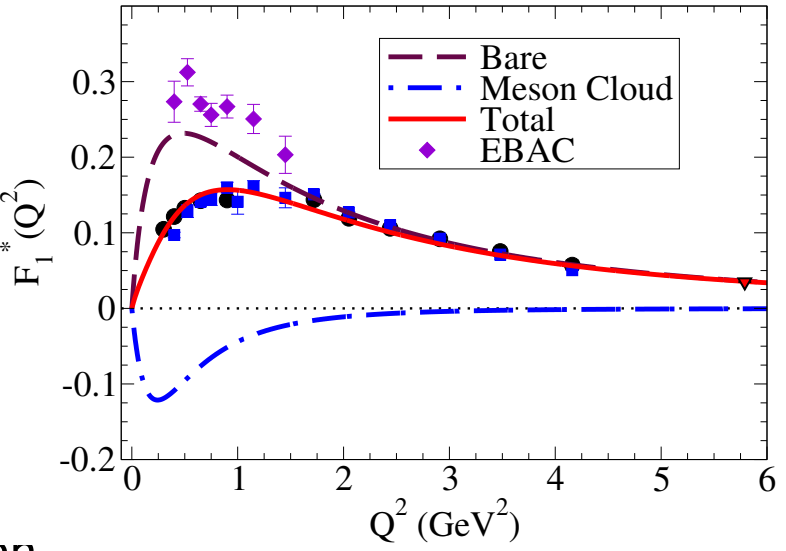


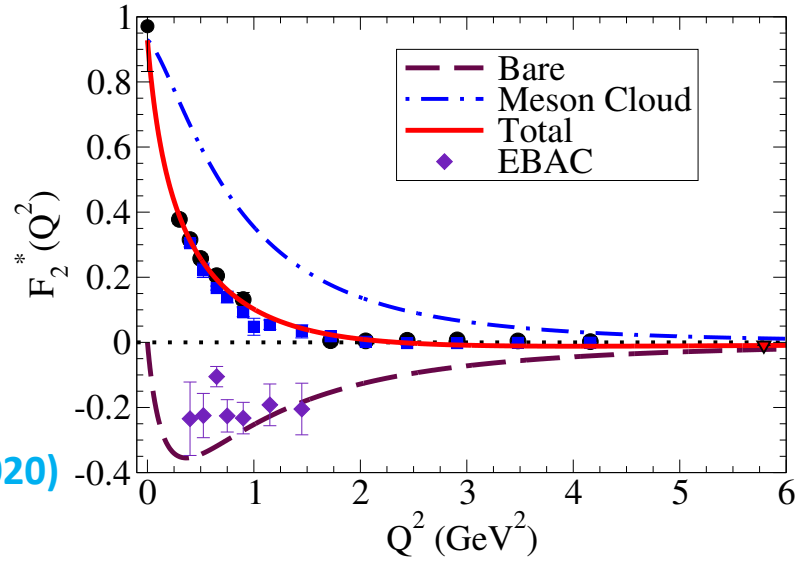


G. Ramalho, M. T. P. , PHYSICAL REVIEW D 101 114008 (2020)

# Extension to the Timelike region

See Izabela Ciepal

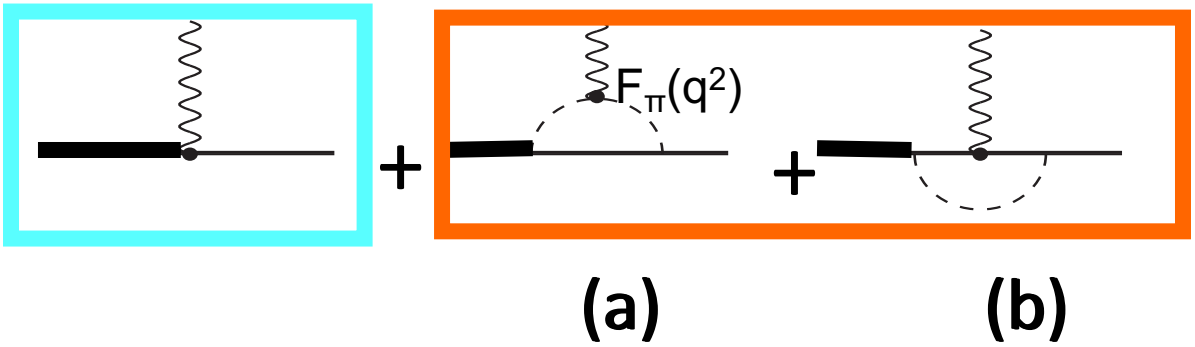


The residue of the pion from factor $F_\pi(q^2)$ at the timelike $\rho$ pole is proportional to the $\rho \longrightarrow \pi\pi$ decay

Diagram (a) related with pion electromagnetic form factor $F_\pi(q^2)$

# Extension to the Timelike region

$\Delta(1232)$ Dalitz decay

Ramalho, Pena, Weil, Van Hees, Mosel,
Phys.Rev. C93 033004 (2016)

$\gamma N \rightarrow \Delta$

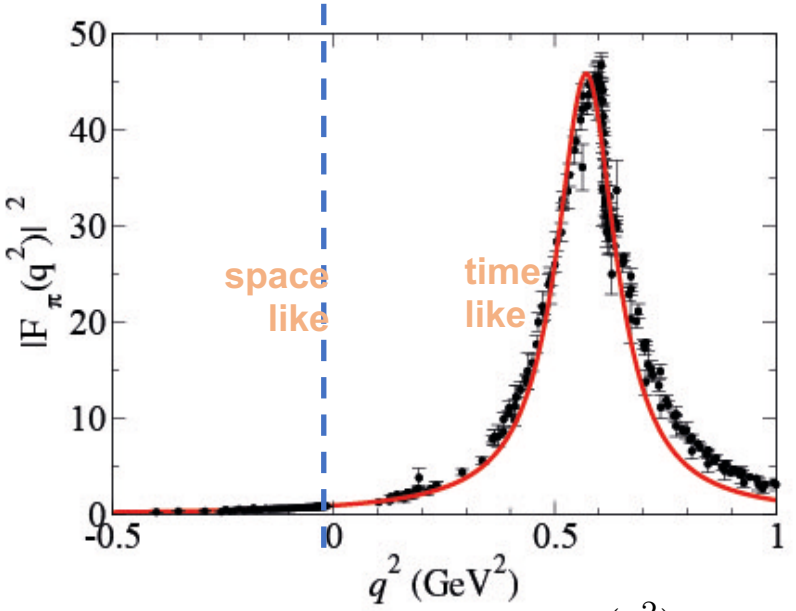


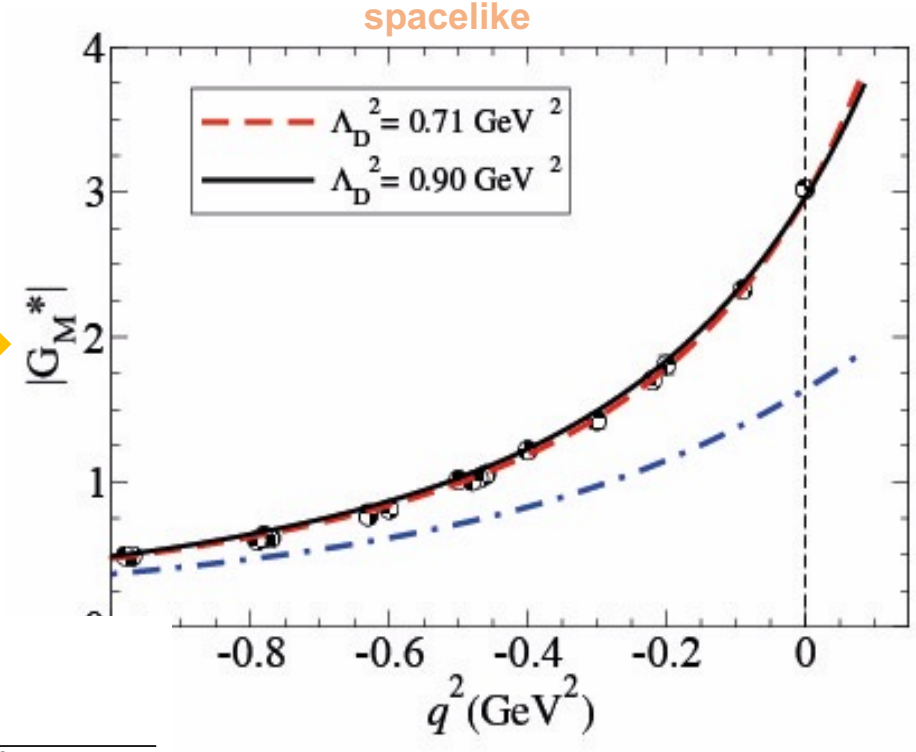


$$F_\pi(q^2) = \frac{\alpha}{\alpha - q^2 - \frac{1}{\pi}\beta q^2 \log\frac{q^2}{m_\pi^2} + i\beta q^2}$$

$\alpha = 0.696$ GeV$^2$

$\beta = 0.178$

Parametrization of pion Form Factor

TFF restricted to the kinematic region that depends on the resonance mass W.

# Dilepton mass spectrum $\Delta(1232)$ Dalitz decay

**HADES Collaboration, Phys.Rev. C95 0652205 (2017)**

proton-proton collisions @1.25 GeV

True CST prediction:
Red line

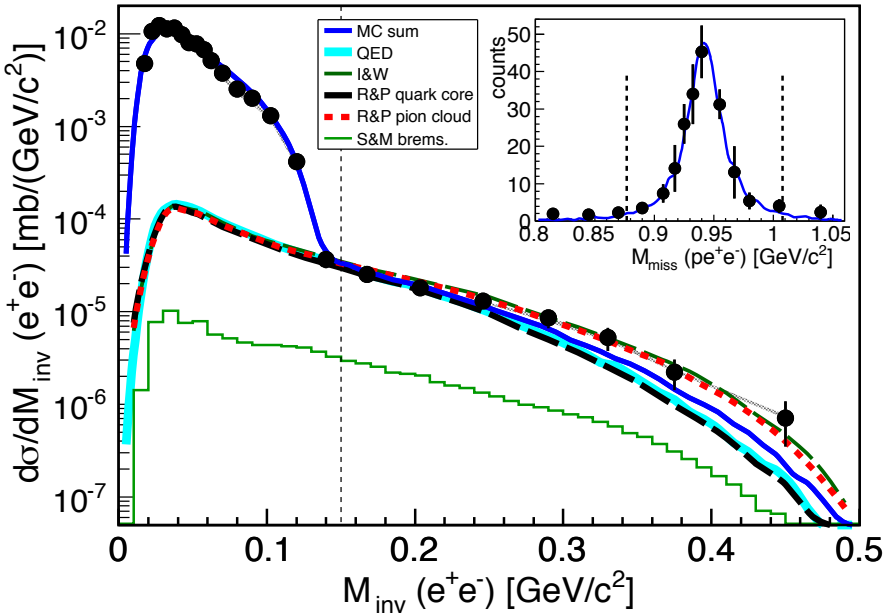


Signature of adequate TFF form factor $q^2$ dependence

$\Delta$ Dalitz decay branching ratio extracted 4.19 x $10^{-5}$

Entry in PDG

$\Gamma(pe^+e^-)/\Gamma_{total}$ $\Gamma_5/\Gamma$

| VALUE (units $10^{-5}$) | DOCUMENT ID |
|---|---|
| **4.19±0.34±0.62** | [1] ADAMCZEW... 17 |

[1] The systematic uncertainty includes the model dependence.

The obtained $\Delta$ Dalitz branching ratio at the pole position is equal to $4.19 \times 10^{-5}$ when extrapolated with the help of the Ramalho-Peña model [27], which is taken as the reference, since it describes the data better. The branching ratio

# Radiative decay widths

N*(1520) $J^P=3/2^-$ I=1/2
60% decay $\pi$ N
30% decay to $\pi\Delta$

Proton

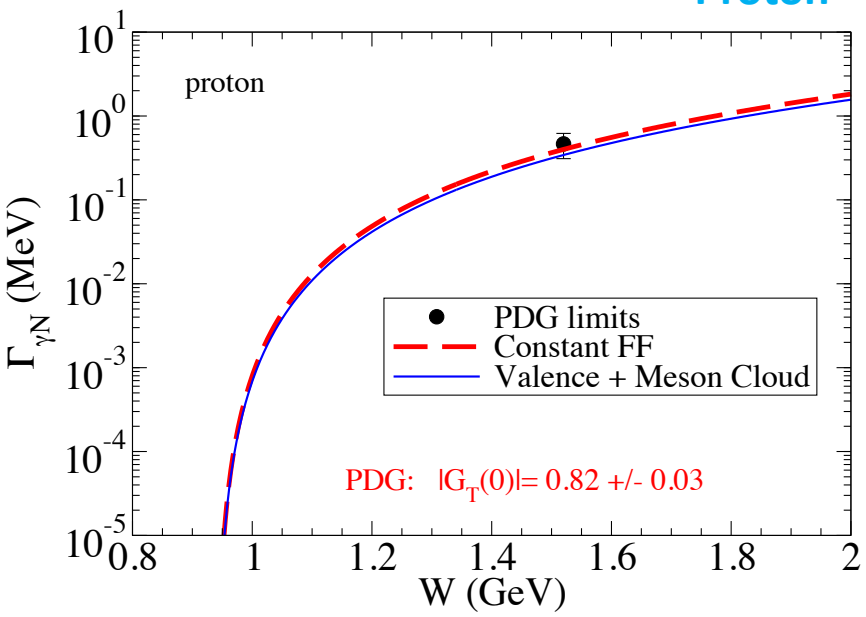


Neutron

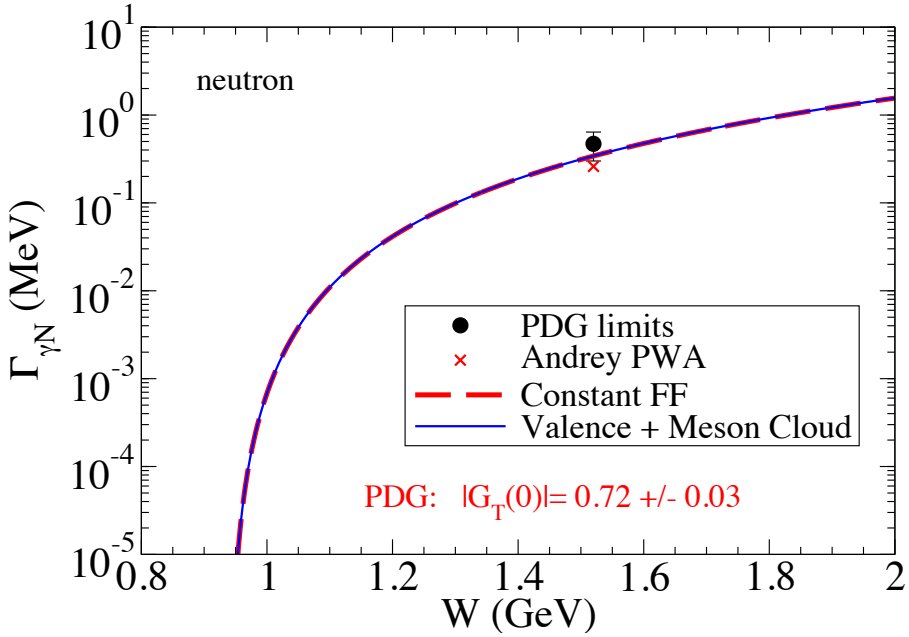


G. Ramalho and M.T. P. Phys. Rev. D 95, 014003 (2017)

Result Consistent with PDG value for $\gamma$N decay width.

# Radiative decay widths

N*(1535) $J^P=1/2^-$ I=1/2

~50% decay to $\pi$ N

~50% decay to $\eta$ N

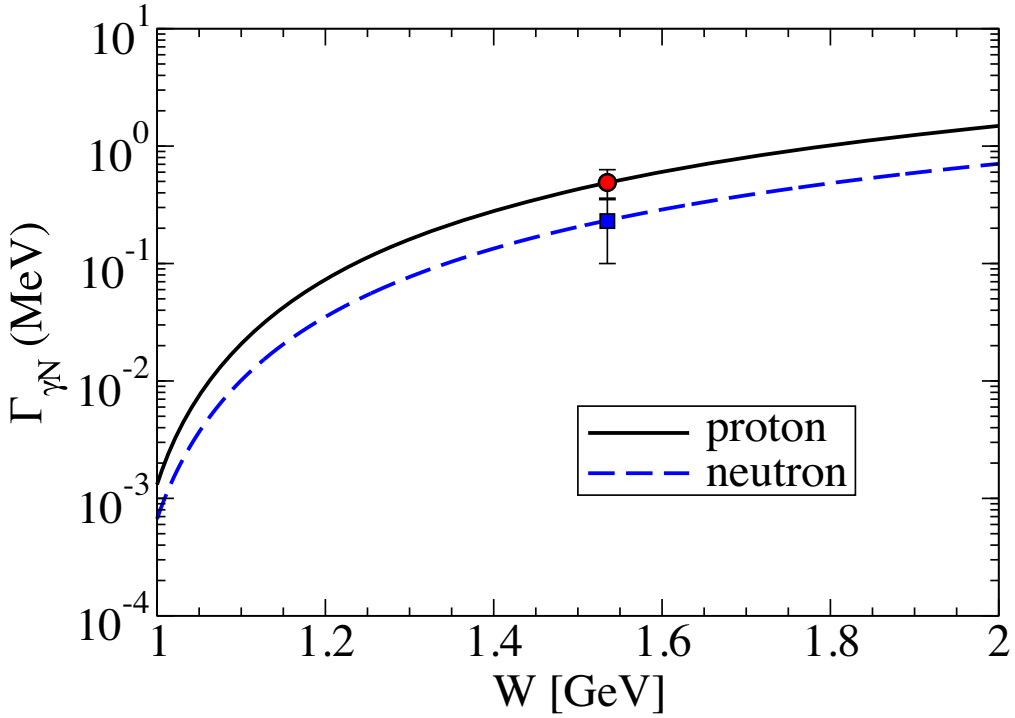


G. Ramalho and M.T. P. Phys.Rev.D 101 (2020) 11, 114008, (2020)

Different results for proton and neutron electromagnetic widths due to iso-scalar term in the eta meson cloud.

Timelike results give information on the neutron.

| | $A_{1/2}(0)$ [GeV$^{-1/2}$] | | $\Gamma_{\gamma N}$ [MeV] | | |
|---|---|---|---|---|---|
| | Data | Model | Estimate | PDG limits | Model |
| $p$ | $0.105 \pm 0.015$ | 0.101 | $0.49 \pm 0.14$ | 0.19–0.53 | 0.503 |
| $n$ | $-0.075 \pm 0.020$ | −0.074 | $0.25 \pm 0.13$ | 0.013–0.44 | 0.240 |

# Dilepton mass spectrum

## N*(1520) + N*(1535)
Dalitz decay

True CST prediction: Red line

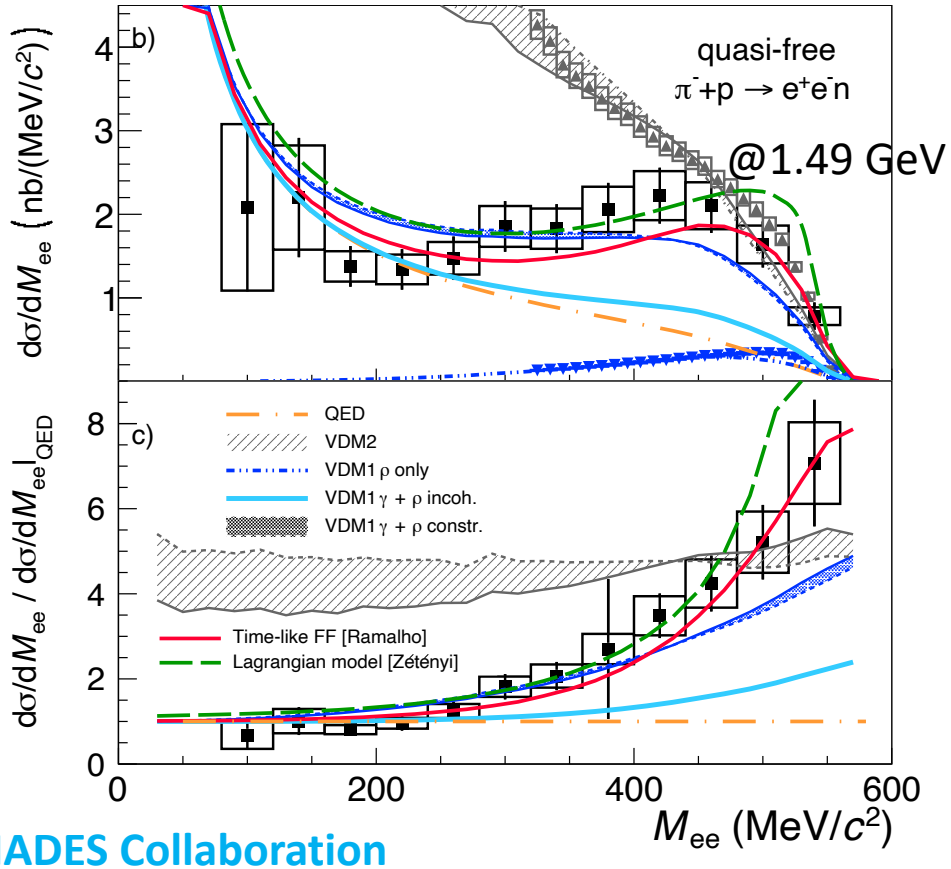


See also talk by Izabela Ciepal

Simulations based on the CST model (**red line**) for these resonances also give a satisfactory description of the data.

Below 200 MeV/$c^2$ , ratio agrees with a pointlike baryon-photon vertex (**QED orange line**) .

At larger invariant masses, data is more than 5 times larger than the pointlike result, showing a strong effect of the transition form factor evolution.

**HADES Collaboration**

"First measurement of massive virtual photon emission from N* baryon resonances" e-Print: 2205.15914 [nucl-ex], 2022

# Inclusive differential cross sections

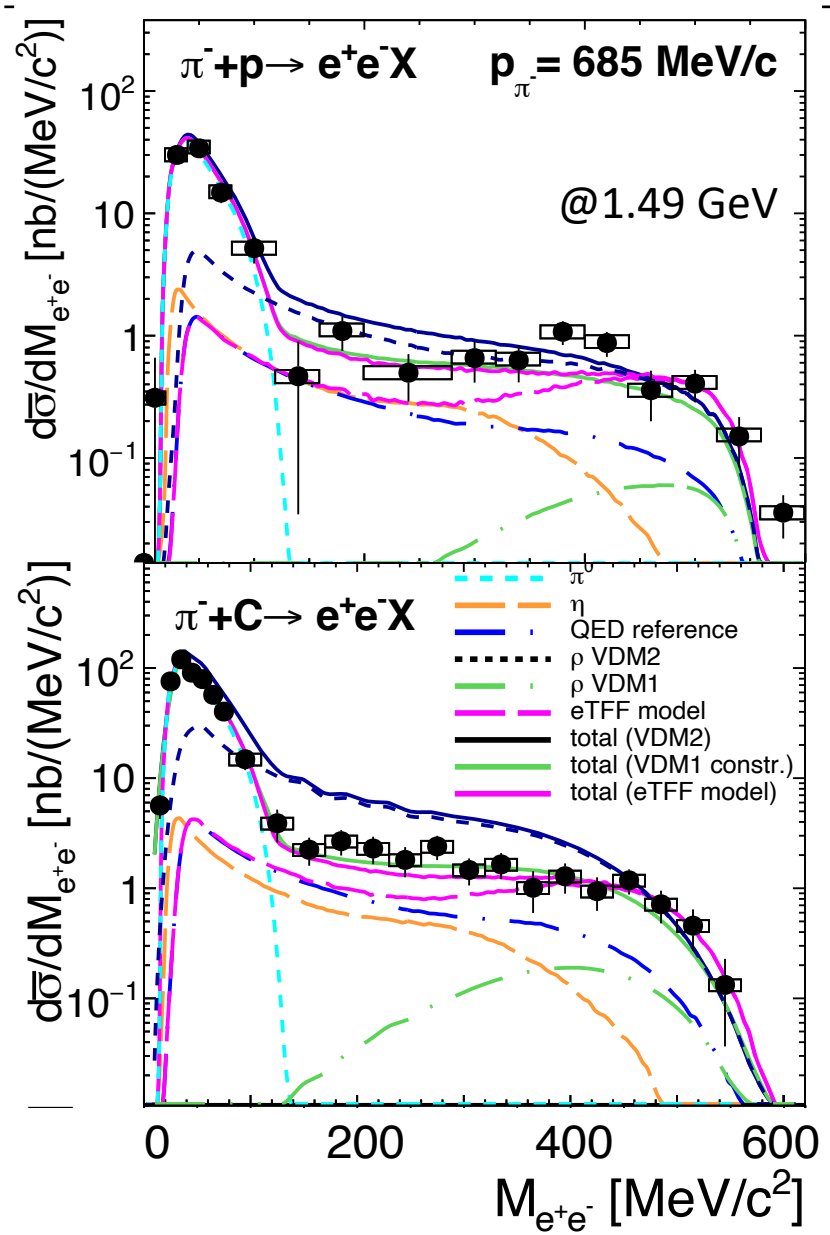


True CST prediction: **Pink** line

**HADES Collaboration**

"Inclusive e+e− production in collisions of pions with protons and nuclei in the second resonance region of baryons"
e-Print 2309.13357 [nucl-ex], 2023

# Extension to the Strange Baryon Sector

Extend the parametrization of the e.m. current to the valence quark d.o.f of the **whole** baryon octet.

$$j_i = \frac{1}{6} f_{i+} \lambda_0 + \frac{1}{2} f_{i-} \lambda_3 + \frac{1}{6} f_{i0} \lambda_s$$

$$\lambda_0 = \begin{pmatrix} 1 & 0 & 0 \\ 0 & 1 & 0 \\ 0 & 0 & 0 \end{pmatrix}, \qquad \lambda_3 = \begin{pmatrix} 1 & 0 & 0 \\ 0 & -1 & 0 \\ 0 & 0 & 0 \end{pmatrix}$$

$$\lambda_s \equiv \begin{pmatrix} 0 & 0 & 0 \\ 0 & 0 & 0 \\ 0 & 0 & -2 \end{pmatrix}$$

Parameters determined by a **global fit** to baryon octed lattice data for the e.m. form factors

**Lattice data:**
**H.W. Lin and K. Orginos, Phys. Rev. D 79, 074507 (2009).**

**G. Ramalho and K.Tsushima, PRD 84, 054014 (2011)**

# CST compared to very recent Hyperon FF data

**Use S.Pacetti, R. Baldini Ferroli and E. Tomasi-Gustafsson, Phys. Rept. 550-551,1 (2015):**

Unitarity and Analyticity demand that for $q^2 \to \infty$

$$G_M(q^2) \simeq G_M^{\rm SL}(-q^2),$$
$$G_E(q^2) \simeq G_E^{\rm SL}(-q^2).$$

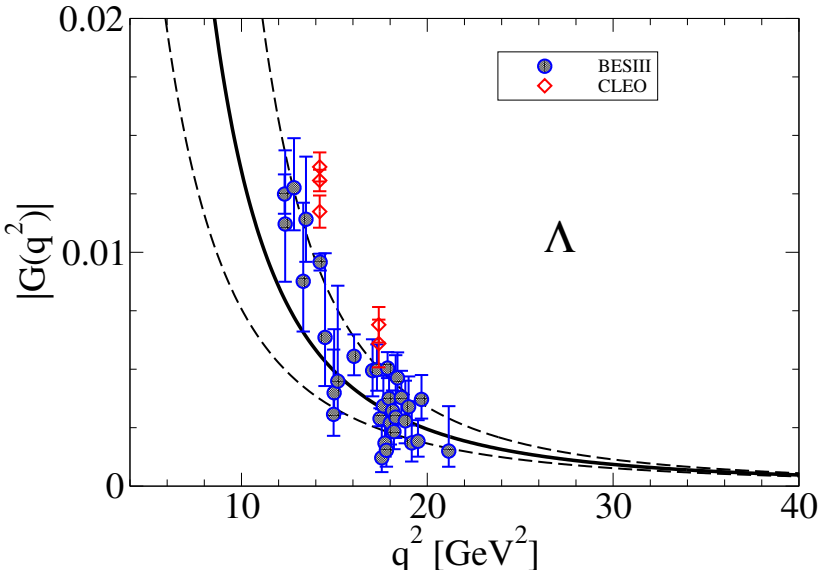


Guidance for determination of onset of ”reflection” symmetry

Uncertainty:

Full line: $G(q^2) = G(2M^2 - q^2)$

Dashed lines: $G(q^2) = G(4M^2 - q^2)$

$G(q^2) = G(-q^2)$

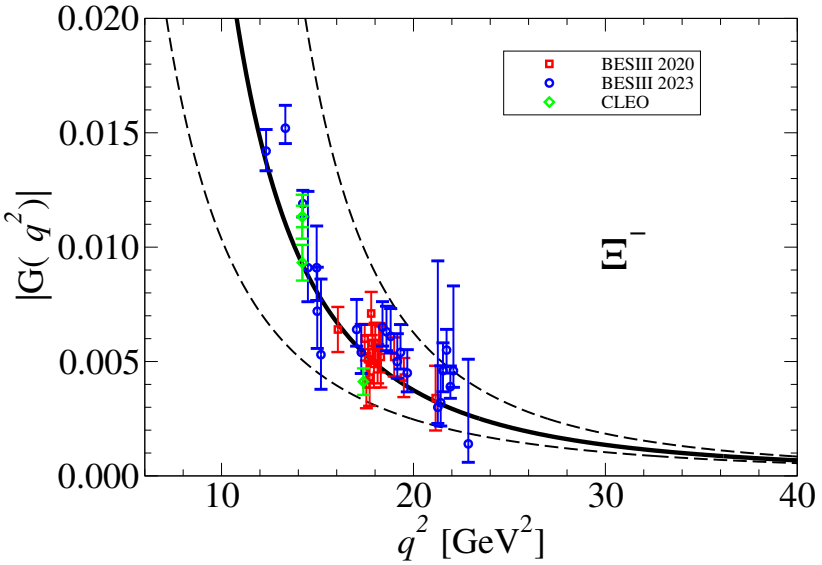

# Summary

**CST** phenomenological ansatz for the baryon wave functions describes

different excited states of the nucleon, with a variety of spin and orbital motion.

Combination with LQCD data is key for predictive power.

**1** Descriptions consistent with spacelike TFF experimental data at high $Q^2=-q^2$;
Spacelike e.m. transition FFs for:
N*(1440), N*(1520), N*(1535), …, baryon octet, etc. (see Gilberto Ramalho talk)

**2** Model made consistent with LQCD in the large pion mass regime through **VMD**.

**3** **VMD** enables also extension to timelike e.m. transition FFs for dilepton mass spectrum and decay widths, and hyperon form factors; predictive power demonstrated.

# Our approach is phenomenological, in the best tradition of the beginnings of Hadron Physics

"Murray looked at two pieces of paper, looked at me and said '***In our field it is costumary to put theory and experiment on the same piece of paper***'."

Memories of Murray and the Quark Model
George Zweig, Int.J.Mod.Phys.A25:3863-3877,2010

Zweig quark or the constituent quark

Back up slides

# How low in Q2 one can go for a partonic interpretation of the meson electroproduction scattering data to be valid?

V. Mokeev, https://userweb.jlab.org/~mokeev/resonance_electrocouplings/

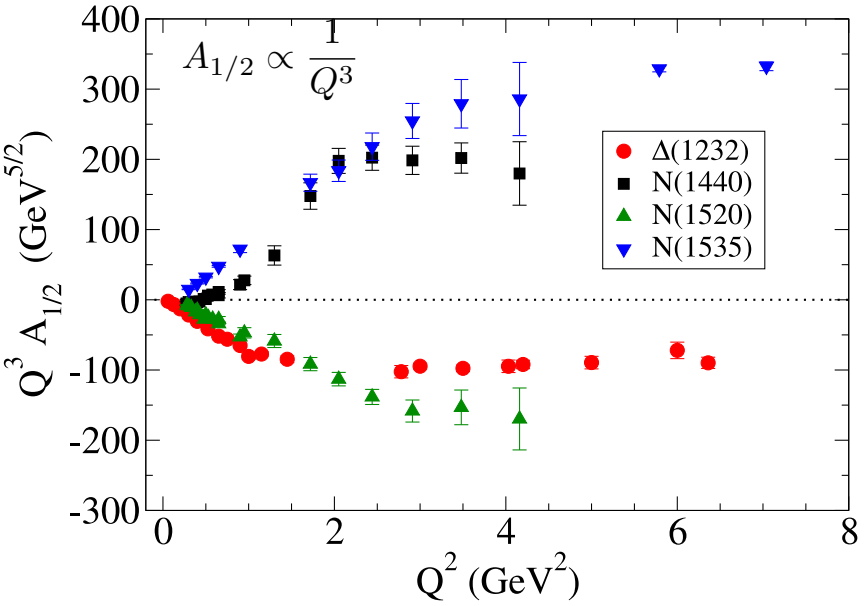


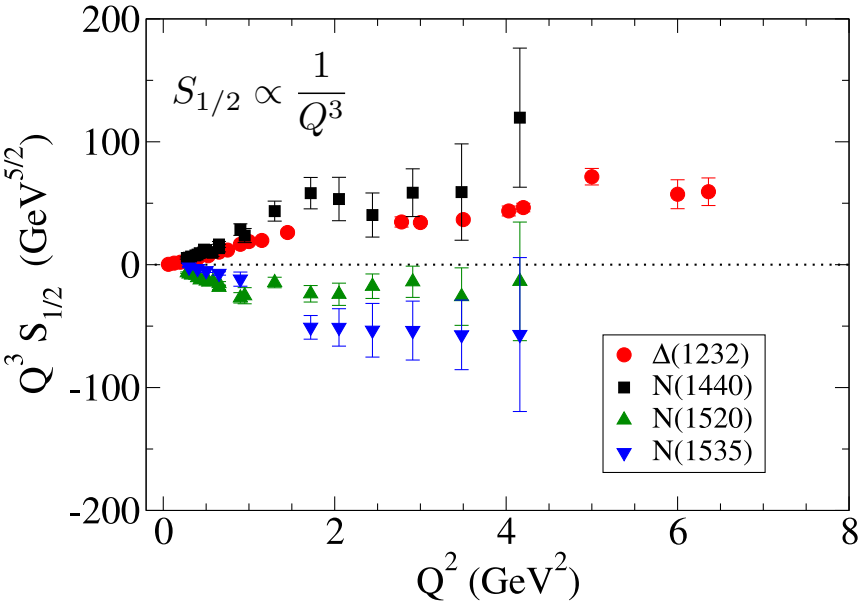


Leading order dependence on Q2

Region Q2 < 2 GeV2 dominated by nonperturbative long-distance multiquark correlations to the resonances;
Higher Q2 region described through single parton processes.

**A.N. Hiller Blin et al.**
**Phys. Rev C 104, 025201 (2021)**

**Application to inclusive nucleon structure functions from exclusive meson electroproduction data**

# E.M. matrix element

**CST©** 2008

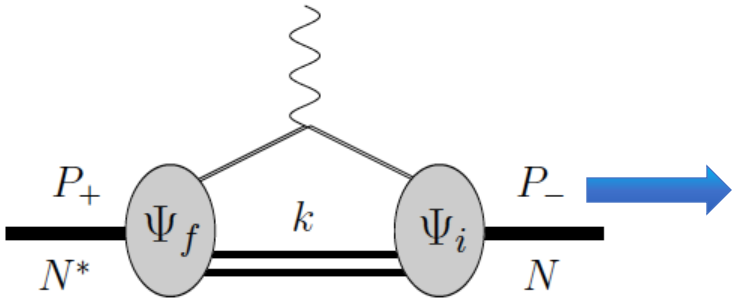


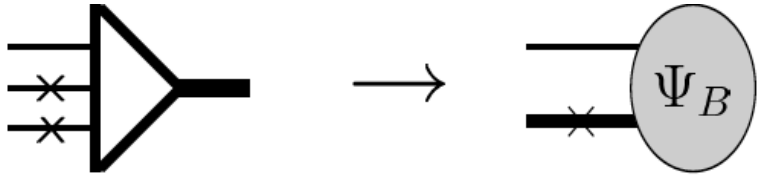


$$\int_{k_1k_2} \equiv \int \frac{d^4k_1 d^4k_2}{(2\pi)^6} \delta_+(m_1^2 - k_1^2)\delta_+(m_2^2 - k_2^2) = \int \frac{d^3k_1 d^3k_2}{(2\pi)^6 4E_1E_2},$$

$$\int_{sk} = \underbrace{\int \frac{d\Omega_{\hat{\mathbf{r}}}}{4(2\pi)^3} \int_{4m_q^2}^{\infty} ds \sqrt{\frac{s-4m_q^2}{s}}}_{\int_s} \underbrace{\int \frac{d^3k}{(2\pi)^3 2E_s}}_{\int_k},$$

- **For the E.M. matrix element calculation,** the Baryon vertex is integrated over the spectator quarks variables.
(Covariant Spectator Model, **CST**)

- **A reduced quark - diquark Baryon** wave function is all that is needed;
it is phenomenologically constructed.

**G. Ramalho, TP, Franz Gross, Phys. Rev. D78, 114017 (2008)**

Uncertainty from range variation of one-gluon exchange interaction width parameter in the infrared region, to which meson and baryon masses are insensitive.

- Relativistic p waves responsible for agreement of $R_{EM}$ with experiment at low Q2

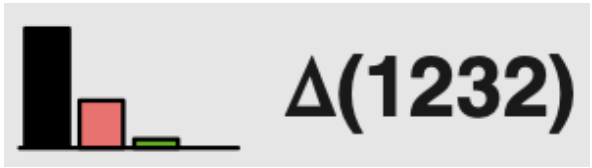


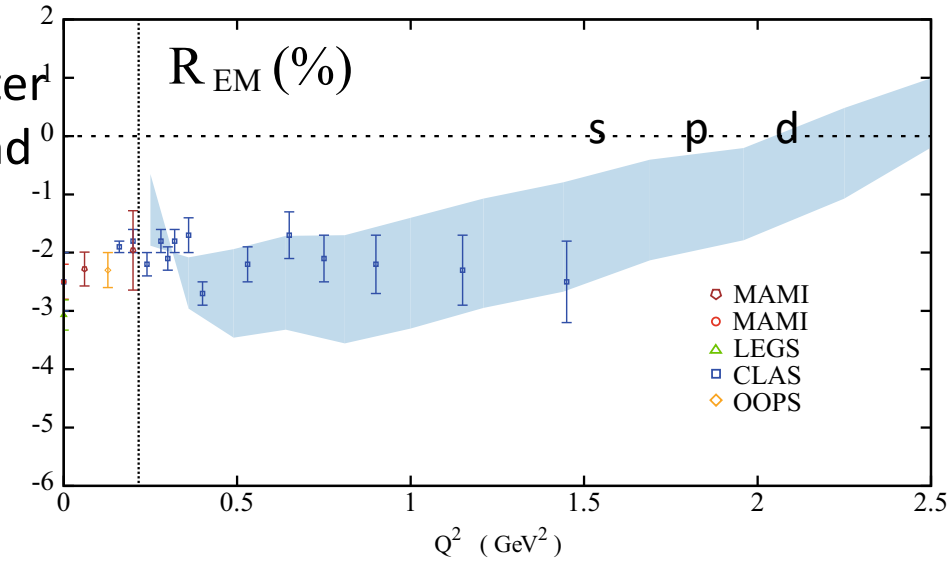


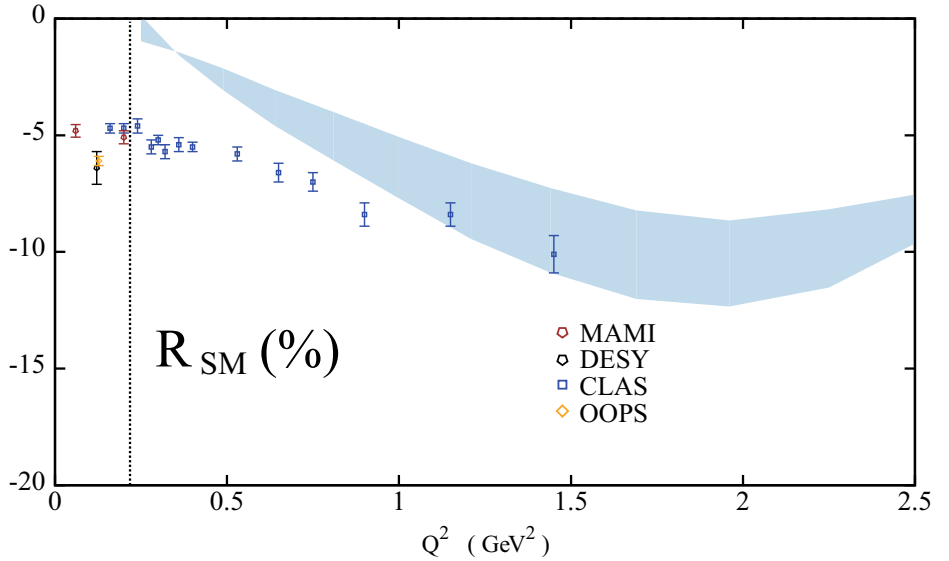


H. Sanchiz-Alepuz, R. Alkofer,C. Fischer Phys. J A (2018) 54

# Extension to the Strange Baryon Sector

Extend the parametrization of the e.m. current to the valence quark d.o.f of the **whole** baryon octet.

$$j_i = \frac{1}{6} f_{i+} \lambda_0 + \frac{1}{2} f_{i-} \lambda_3 + \frac{1}{6} f_{i0} \lambda_s$$

$$\lambda_0 = \begin{pmatrix} 1 & 0 & 0 \\ 0 & 1 & 0 \\ 0 & 0 & 0 \end{pmatrix}, \qquad \lambda_3 = \begin{pmatrix} 1 & 0 & 0 \\ 0 & -1 & 0 \\ 0 & 0 & 0 \end{pmatrix}$$

$$\lambda_s \equiv \begin{pmatrix} 0 & 0 & 0 \\ 0 & 0 & 0 \\ 0 & 0 & -2 \end{pmatrix}$$

Parameters determined by a **global fit** to octet baryon lattice data for the e.m. form factors and physical magnetic moments.

**Lattice data:**
**H.W. Lin and K. Orginos, Phys. Rev. D 79, 074507 (2009).**

Two examples:

**Red** line: lattice
**Blue** line: physical regime

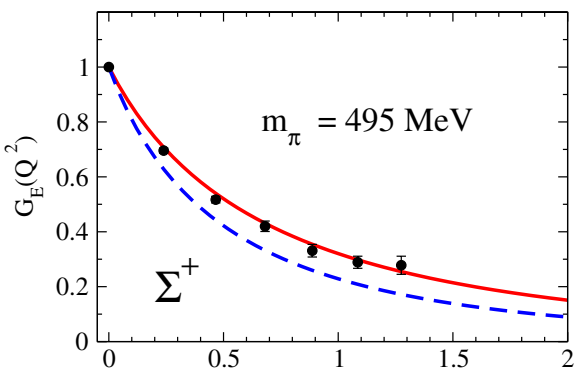


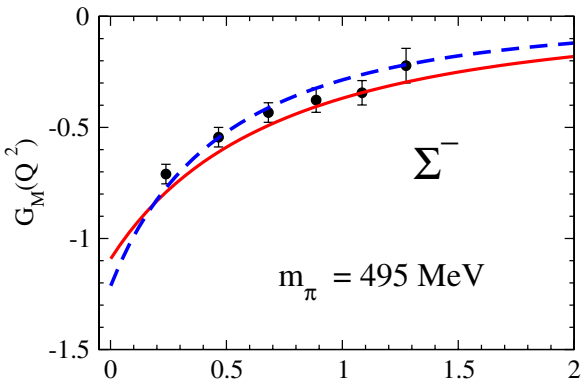


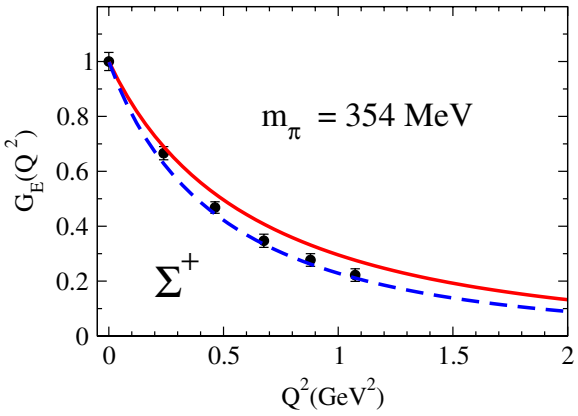


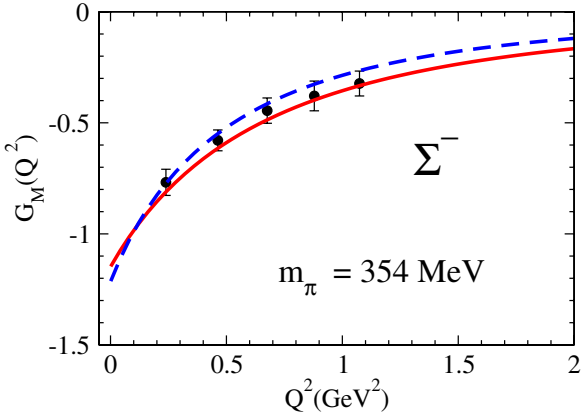


**G. Ramalho and K.Tsushima, PRD 84, 054014 (2011)**

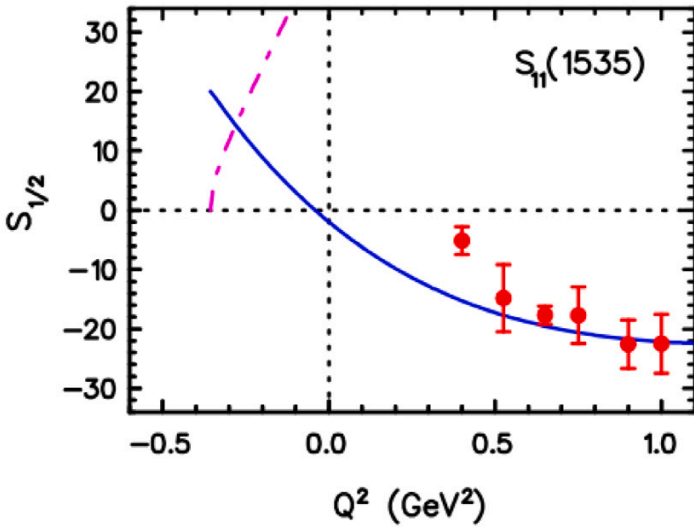
S11(1535)
S1/2
Q² (GeV²)

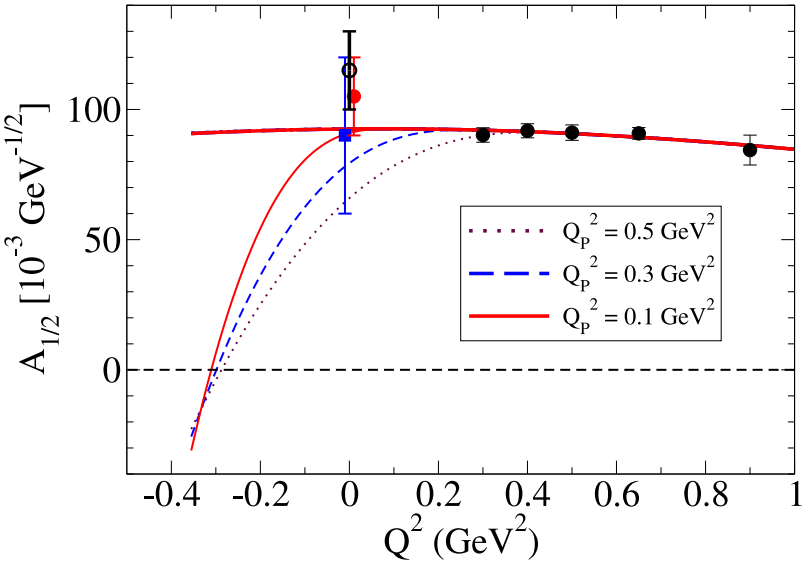
A1/2 [10-3 GeV-1/2]
Q2 (GeV2)
QP2 = 0.5 GeV2
QP2 = 0.3 GeV2
QP2 = 0.1 GeV2

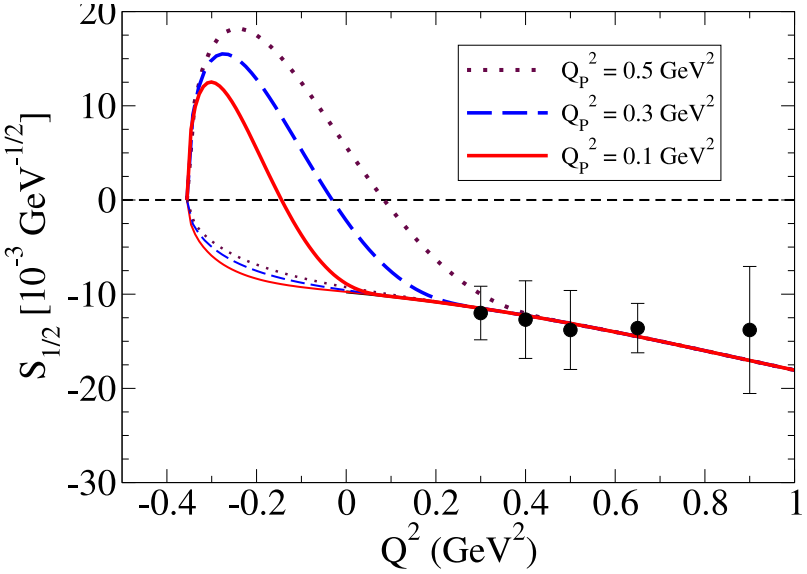
S1/2 [10-3 GeV-1/2]
Q2 (GeV2)
QP2 = 0.5 GeV2
QP2 = 0.3 GeV2
QP2 = 0.1 GeV2

# Post 2020 Hyperon data evolution

| | $G$ | $\frac{G_E}{G_M}$ | $\Delta\Phi$ | Experiment | $q^2$ range ($\mathrm{GeV}^2$) |
|---|---|---|---|---|---|
| $\Lambda$ | √ | | | BESIII23 [13] | 5.0–8.7 |
| | √ | | | BESIII21 [16] | 12.3–21.2 |
| | √ | | | BaBar06 [8], CLEO [31, 32] | |
| | | √ | √ | BESIII22 [15] | 14.2 |
| | | √ | √ | BESIII23 [14] | 13.8 † |
| | √ | √ | √ | BESIII19 [22] | 5.7 |
| | √ | √ | | BaBar07 [9] | |
| $\Sigma^+$ | √ | √ | √ | BESIII23 [10] | 5.7–8.4 |
| | √ | √ | | BESIII21 [19] | 5.7–9.1 |
| | √ | | | CLEO [31, 32] | |
| $\Xi^-$ | √ | | | BESIII23 [11] | 9.6–23.5 |
| | √ | | | BESIII20 [21] | 16.1–21.2 |

$$\left|\mathrm{Re}\left(\frac{G_E}{G_M}\right)\right| = \frac{|G_E|}{|G_M|}|\cos(\Delta\Phi)|,$$

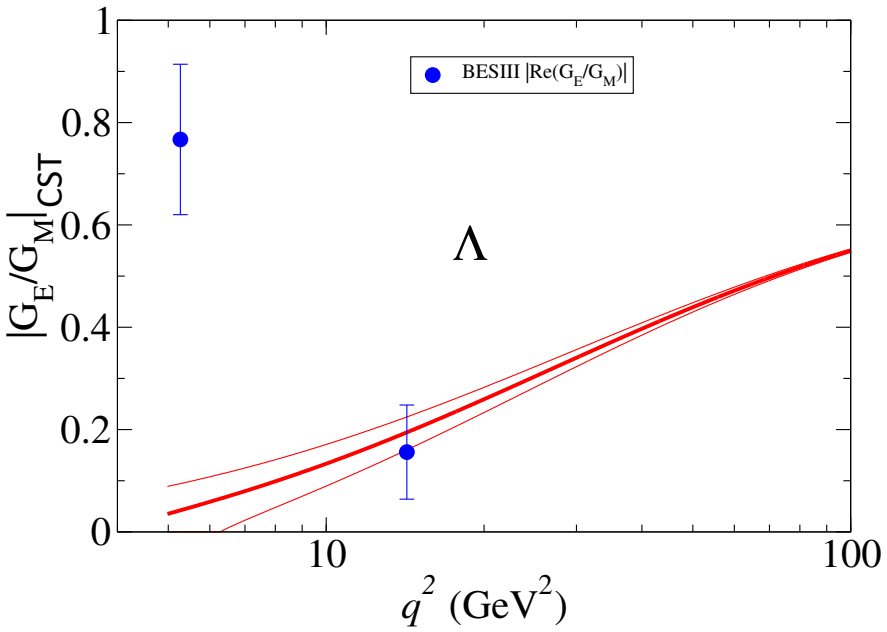


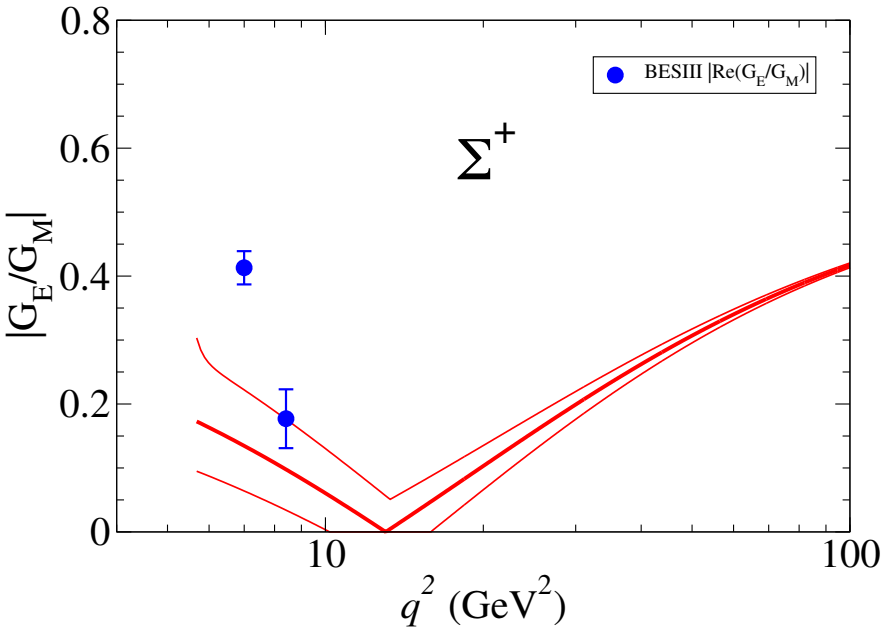

DS-BS calculations with a ladder kernel given by dressed one-gluon exchange

$$K_a^{(2)} = Z_2^2 \frac{4\pi\alpha_{eff}(k^2)}{k^2} T^{\mu\nu}(k)\gamma_\mu\gamma_\nu$$

Running Strong coupling constant

$$\alpha_{\rm eff}(k^2) = \pi\eta^7 \left(\frac{k^2}{\Lambda^2}\right)^2 e^{-\eta^2 \frac{k^2}{\Lambda^2}} + \frac{2\pi\gamma_m(1-e^{-k^2/\Lambda_t^2})}{\ln[e^2 - 1 + (1+k^2/\Lambda_{QCD}^2)^2]}$$

Uncertainty band $1.6 < \eta < 2$

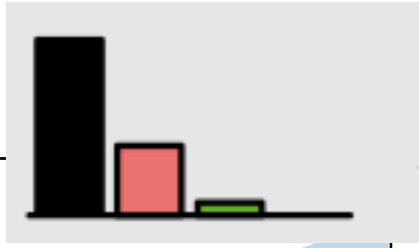

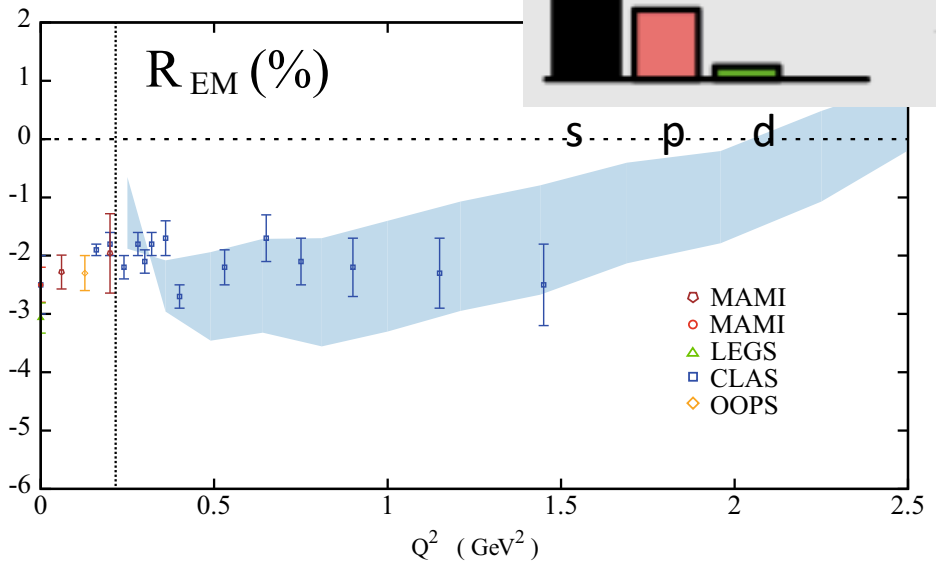


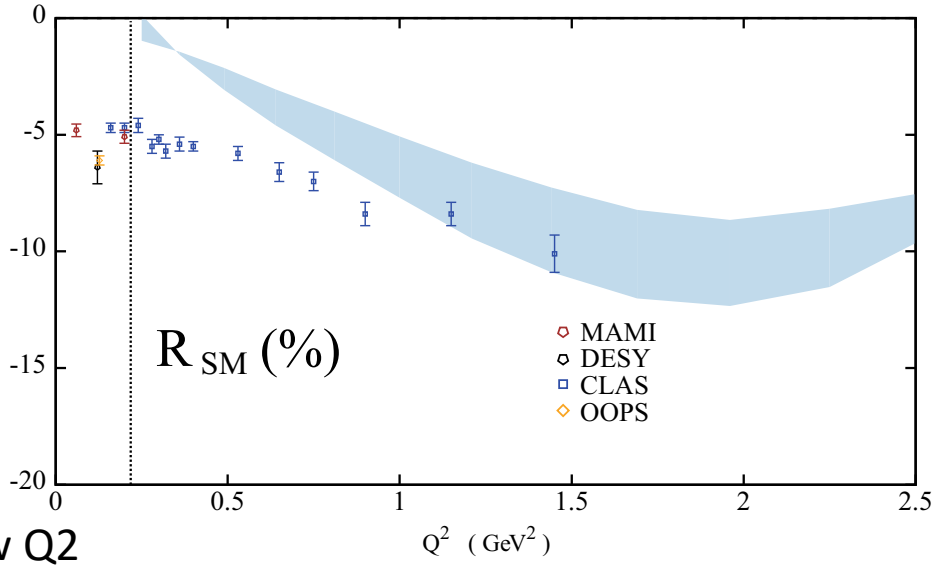


- There is the potential for narrowing down this uncertainty in the Kernel.
- Technically, calculations limited to a Q2 window due to the timelike singularities of the quark propagator nearest to the spacelike region
- Relativistic p waves responsible for agreement of $R_{EM}$ with experiment at low Q2

H. Sanchiz-Alepuz, R. Alkofer,C. Fischer Phys. J A (2018) 54

- ✓ The wf is symmetry based only; not dynamically generated
- ✓ The Diquark is not pointlike; it encloses structure

Eg. S-wave

- **Nucleon** wavefunction

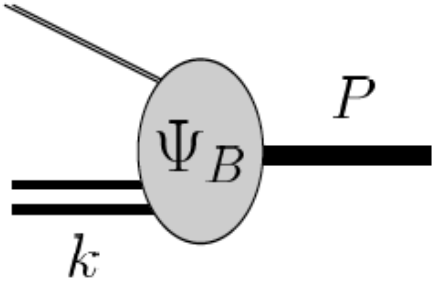


- A quark + **scalar**-diquark component
- A quark+ **axial vector**-diquark component

$$\Psi^S_{N\lambda_n}(P,k) = \frac{1}{\sqrt{2}}[\phi^0_I u_N(P,\lambda_n) - \phi^1_I \varepsilon^{\alpha *}_{\lambda P} U_\alpha(P,\lambda_n)] \times \psi^S_N(P,k)$$

$$U_\alpha(P,\lambda_n) = \frac{1}{\sqrt{3}}\gamma_5\left(\gamma_\alpha - \frac{P_\alpha}{m_H}\right)u_N(P,\lambda_n),$$

Phenomenological functions $\psi$

- ✓ The wf is symmetry based only; not dynamically generated
- ✓ The Diquark is not pointlike; it encloses structure

Eg. S-wave

- **Nucleon** wavefunction

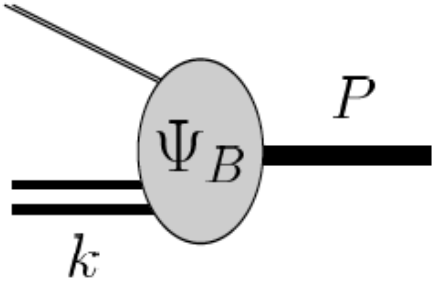


  - A quark + **scalar**-diquark component
  - A quark+ **axial vector**-diquark component

$$\Psi^S_{N\lambda_n}(P,k) = \frac{1}{\sqrt{2}}[\phi^0_I u_N(P,\lambda_n) - \phi^1_I \varepsilon^{\alpha *}_{\lambda P} U_\alpha(P,\lambda_n)] \times \psi^S_N(P,k)$$

- **Delta (1232)** "wavefunction"

$$U_\alpha(P,\lambda_n) = \frac{1}{\sqrt{3}}\gamma_5\left(\gamma_\alpha - \frac{P_\alpha}{m_H}\right)u_N(P,\lambda_n),$$

  - Only quark + **axial vector**-diquark term contributes

Phenomenological functions $\psi$

$$\Psi^S_\Delta(P,k) = -\psi^S_\Delta(P,k)\tilde{\phi}^1_I \varepsilon^{\beta *}_{\lambda P} w_\beta(P,\lambda_\Delta)$$

| | | |
|---|---|---|
| $A_{1/2} \propto \|\mathbf{q}\|,$ | $S_{1/2} \propto \|\mathbf{q}\|^2$ | |
| $A_{1/2} \propto 1,$ | $S_{1/2} \propto \|\mathbf{q}\|$ | $A_{1/2} = \sqrt{2}(M_R - M)\frac{S_{1/2}}{\|\mathbf{q}\|}$ |
| $A_{1/2} \propto \|\mathbf{q}\|,$ | $S_{1/2} \propto \|\mathbf{q}\|^2$ | $\left(A_{1/2} - \frac{1}{\sqrt{3}}A_{3/2}\right)\frac{1}{\|\mathbf{q}\|} = \sqrt{2}(M_R - M)\frac{S_{1/2}}{\|\mathbf{q}\|^2}$ |
| $A_{3/2} \propto \|\mathbf{q}\|$ | | |
| $A_{1/2} \propto 1,$ | $S_{1/2} \propto \|\mathbf{q}\|$ | |
| $A_{3/2} \propto 1$ | | |

Safer to use the general forms of the offshell nucleon-to-resonance transition vertices that implement electromagnetic and spin-3/2 gauge invariance,
and automatically define on-shell transition form factors free of kinematic constraints.

Gernot Ecihmann and Gilbeto Ramalho Phys. Rev. D 98, 093007 (2018)

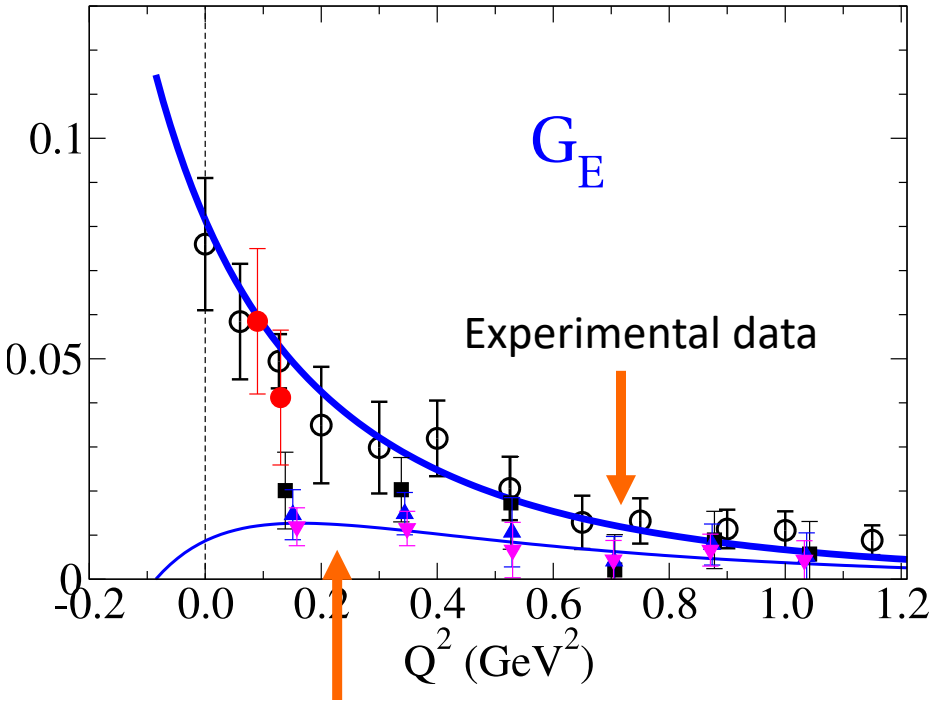


Quenched Lattice data

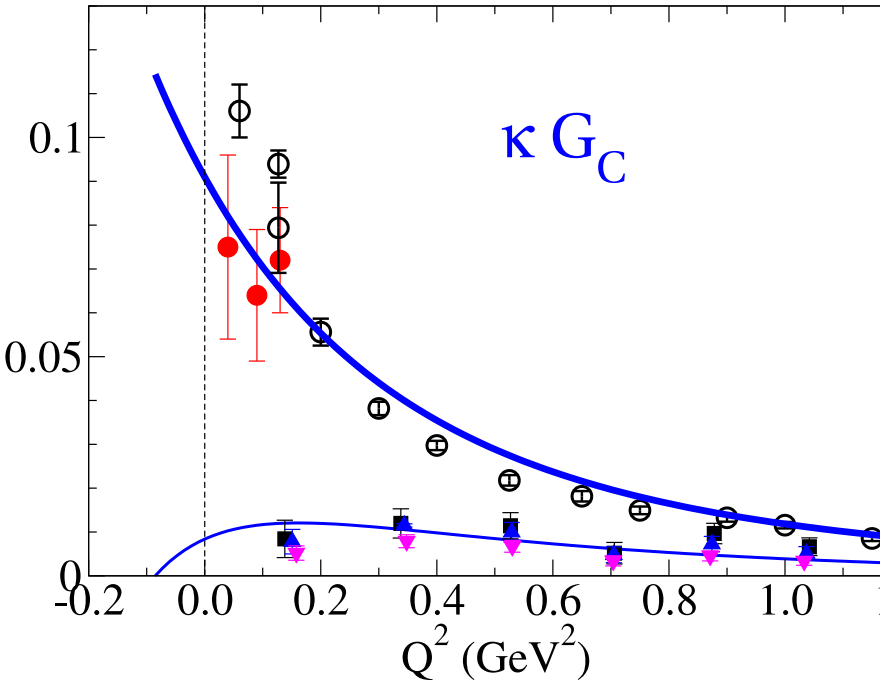

$$f(Q^2) = e + gB(Q^2)e + gB(Q^2)gB(Q^2)e + \cdots = e + \frac{gB(Q^2)e}{1 - gB(Q^2)}$$

if $gB(Q^2) = \frac{\lambda^2}{\Lambda^2 + Q^2}$, then $f(Q^2) = e + \frac{\lambda^2 e}{\Lambda^2 - \lambda^2 + Q^2}$

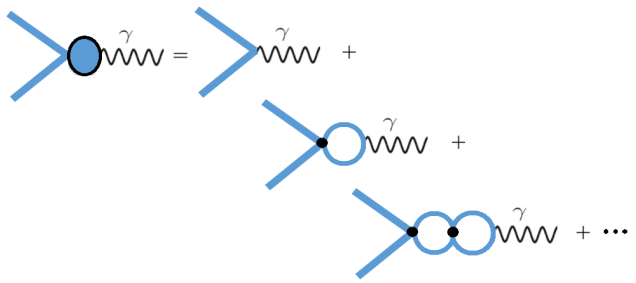

$$\Gamma_\mu(p,Q) = \gamma_\mu + \int \frac{d^4q}{(2\pi)^4} K(p,q,Q) S(q+\eta Q) \Gamma_\mu(q,Q) S(q-\eta Q)$$

$$f_{1+} = \lambda + \frac{1-\lambda}{1+Q_0^2/m_v^2} + \frac{c_\pm Q_0^2/M_h^2}{\left(1+Q_0^2/M_h^2\right)^2}$$

$$f_{2\pm} = \kappa_\pm \left( \frac{d_\pm}{1+Q_0^2/m_v^2} + \frac{(1-d_\pm)}{1+Q_0^2/M_h^2} \right)$$

To parametrize the current use Vector Meson Dominance at the quark level a truncation to the rho and omega poles of the full meson spectrum contribution to the quark-photon coupling.

**4** parameters

$$\frac{m_v^2}{m_v^2 - q^2} \rightarrow \frac{m_v^2}{m_v^2 - q^2 - i m_v \Gamma_v(q^2)},$$

$$\Gamma_\rho(q^2) = \Gamma_\rho^0 \frac{m_\rho^2}{q^2} \left( \frac{q^2 - 4m_\pi^2}{m_\rho^2 - 4m_\pi^2} \right)^{\frac{3}{2}} \theta(q^2 - 4m_\pi^2), \quad (4.7)$$

where $\Gamma_\rho^0 = 0.149$ GeV.

For the application in this paper, however, we also have to include the $\omega$ pole. To this end, the function $\Gamma_\omega(q^2)$ will include the decays $\omega \to 2\pi$ (function $\Gamma_{2\pi}$) and $\omega \to 3\pi$ (function $\Gamma_{3\pi}$). The case $\omega \to 3\pi$ can be interpreted as the process $\omega \to \rho\pi \to 3\pi$, and therefore we decomposed $\Gamma_\omega(q^2)$ into [44]

$$\Gamma_\omega(q^2) = \Gamma_{2\pi}(q^2) + \Gamma_{3\pi}(q^2), \quad (4.8)$$

$$\Gamma_{2\pi}(q^2) = \Gamma_{2\pi}^0 \frac{m_\omega^2}{q^2} \left( \frac{q^2 - 4m_\pi^2}{m_\omega^2 - 4m_\pi^2} \right)^{\frac{3}{2}} \theta(q^2 - 4m_\pi^2), \quad (4.9)$$

where $\Gamma_{2\pi}^0 = 1.428 \times 10^{-4}$ GeV. Note that $\Gamma_{2\pi}$ is similar to the function $\Gamma_\rho$ except for the constant $\Gamma_{2\pi}^0$ (about $10^3$ smaller) and the mass. For the function $\Gamma_{3\pi}$ we use the result from Ref. [44]

$$\Gamma_{3\pi}(q^2) = \int_{9m_\pi^2}^{(q-m_\pi)^2} ds\, \mathcal{A}_\rho(s) \bar{\Gamma}_{\omega\to\rho\pi}(q^2, s), \quad (4.10)$$

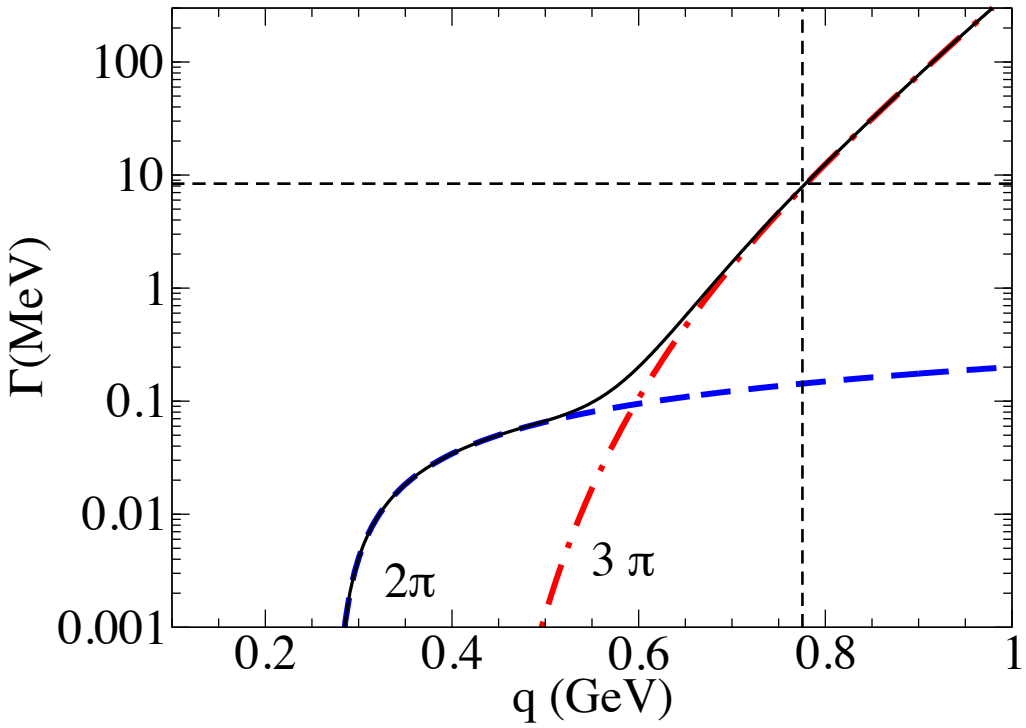


FIG. 1: $\Gamma_\omega$ as a function of $q$. The $2\pi$, $3\pi$ channels are indicated by the long-dashed and dotted-dashed lines respectively. The solid line represents the sum of the two channels. The short-dashed vertical and horizontal lines indicate the $\omega$ mass point and the $\omega$-physical width (8.4 MeV).

# Extension to Strangeness in the timelike region

CST seems to work well at large $Q^2$.

$$e^+e^- \to \gamma^* \to B\bar{B}$$

**Use S.Pacetti, R. Baldini Ferroli and E. Tomasi-Gustafsson, Phys. Rept. 550-551,1 (2015).**

Unitarity and Analyticity demand that for $q^2 \to \infty$

Reflection symmetry sets in, implying real form factor as in the space like region

$$G_M(q^2) \simeq G_M^{\rm SL}(-q^2),$$
$$G_E(q^2) \simeq G_E^{\rm SL}(-q^2).$$

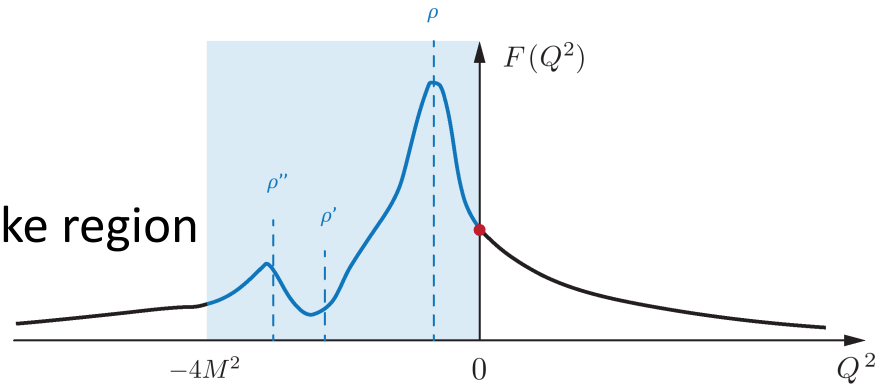


Effective Form factor that gives the integrated cross section

$$|G(q^2)|^2 = \left(1+\frac{1}{2\tau}\right)^{-1}\left[|G_M(q^2)|^2 + \frac{1}{2\tau}|G_E(q^2)|^2\right]$$
$$= \frac{2\tau|G_M(q^2)|^2 + |G_E(q^2)|^2}{2\tau+1}.$$

$$\tau = \frac{q^2}{4M_B^2}$$

$$\Gamma_{\gamma^* N}(q;W) = \frac{\alpha}{16}\frac{(W+M)^2}{M^2 W^3}\sqrt{y_+ y_-}\, y_- |G_T(q^2,W)|^2$$

$$|G_T(q^2;M_\Delta)|^2 = |G_M^*(q^2;W)|^2 + 3|G_E^*(q^2;W)|^2 + \frac{q^2}{2W^2}|G_C^*(q^2;W)|^2$$

$$y_\pm = (W \pm M)^2 - q^2$$

$$\Gamma_{\gamma N}(W) \equiv \Gamma_{\gamma^* N}(0;W)$$

$$\Gamma_{e^+e^- N}(W) = \frac{2\alpha}{3\pi}\int_{2m_e}^{W-M} \Gamma_{\gamma^* N}(q;W)\frac{dq}{q}$$

# $N \to N^*(1440)$ **TFFs**

$J^P=1/2^+$ $I=1/2$

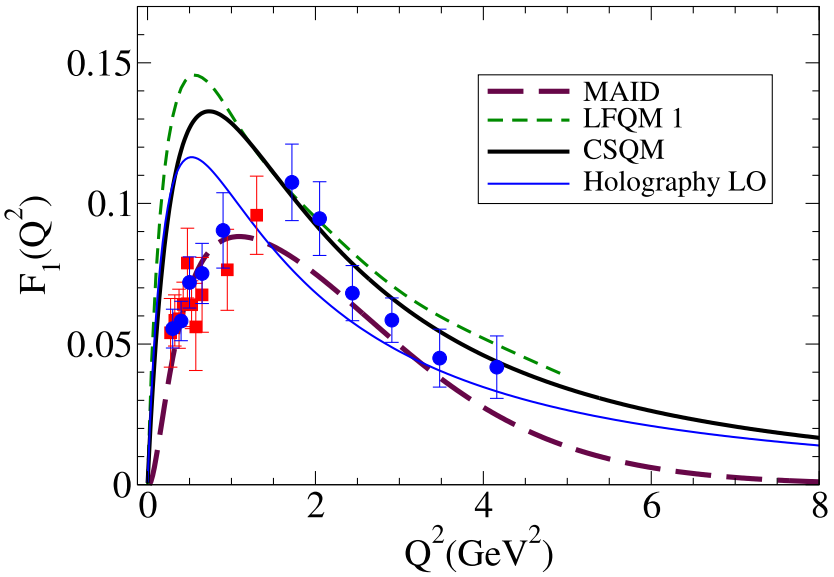


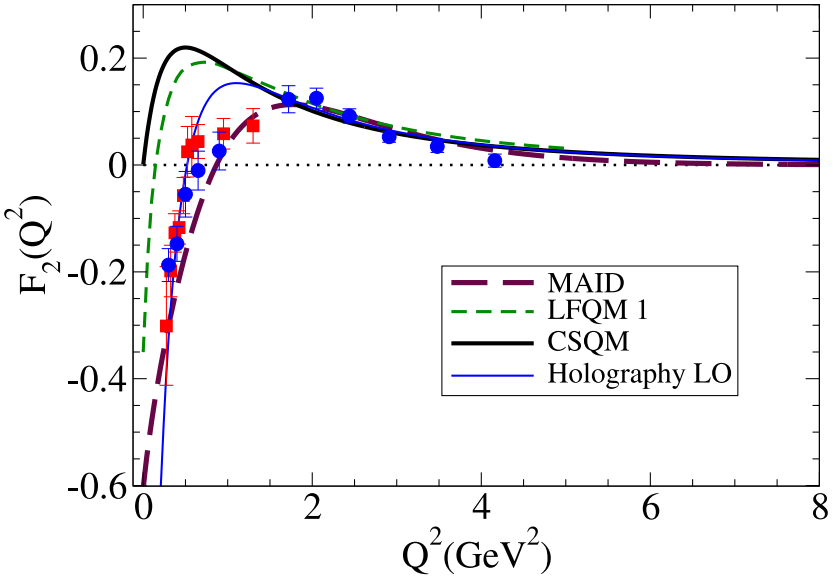


G. Ramalho, M. T. P. , Prog. Part. Nucl. Phys., 2023

# Extension to Timelike

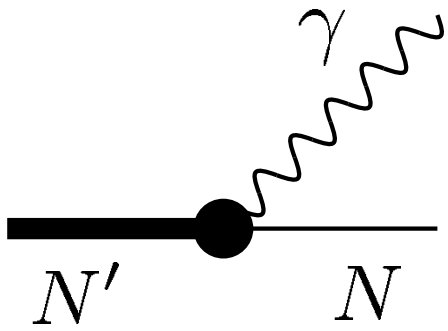


$R$ rest frame

$P_R = (W, 0, 0, 0); \quad P_N = (E_N, 0, 0, -|\mathbf{q}|); \quad q = (\omega, 0, 0, |\mathbf{q}|)$

Timelike $q^2 > 0$

$$\omega = \frac{W^2 - M^2 + q^2}{2W}$$

$$|\mathbf{q}|^2 = \frac{[(W+M) - q^2][(W-M)^2 - q^2]}{4W^2}$$

$$E_N = \frac{W^2 + M^2 - q^2}{2W}$$

TL: $q^2 \leq (W - M)^2$

Spacelike $-q^2 = Q^2 > 0$

$$\omega = \frac{W^2 - M^2 - Q^2}{2W}$$

$$|\mathbf{q}|^2 = \frac{[(W+M) + Q^2][(W-M)^2 + Q^2]}{4W^2}$$

$$E_N = \frac{W^2 + M^2 + Q^2}{2W}$$

$W \geq M$

Transition form factors in the timelike region are restricted to a given kinematic region that depends on the varying resonance mass W.

# Extension to Strangeness in the timelike region

$e^+e^- \to \gamma^* \to B\bar{B}$

Data from Babar, CLEO,BESIII

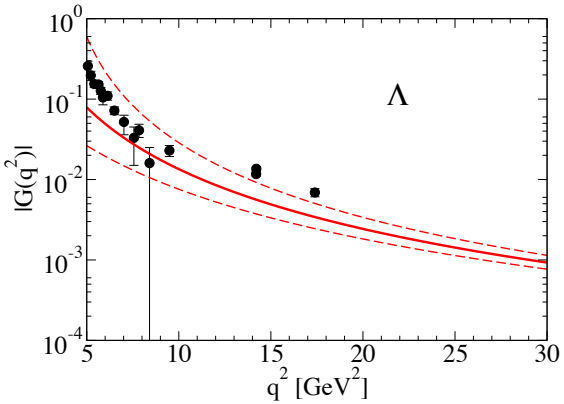


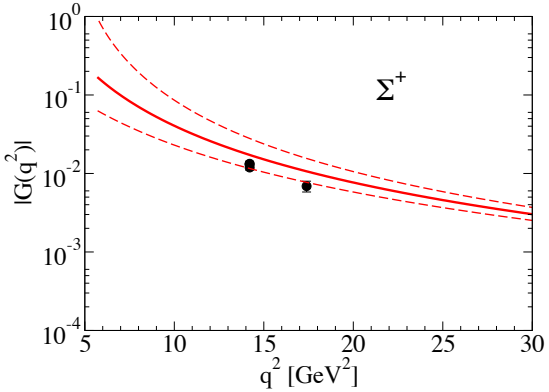


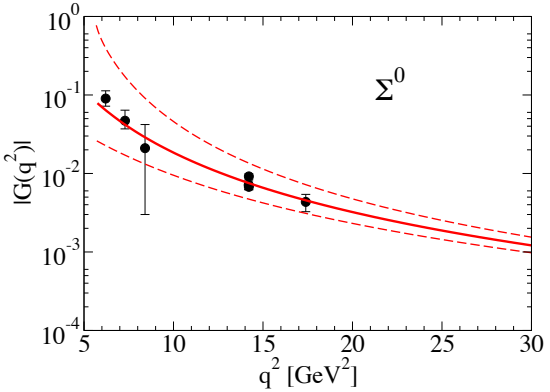


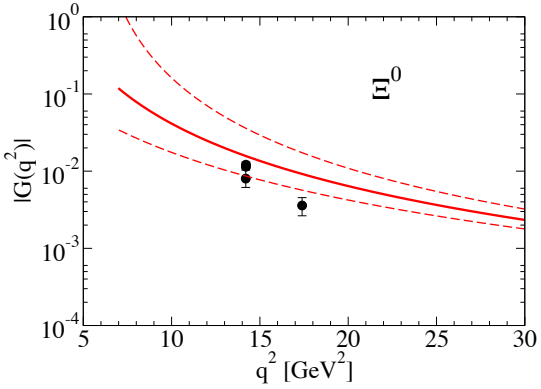


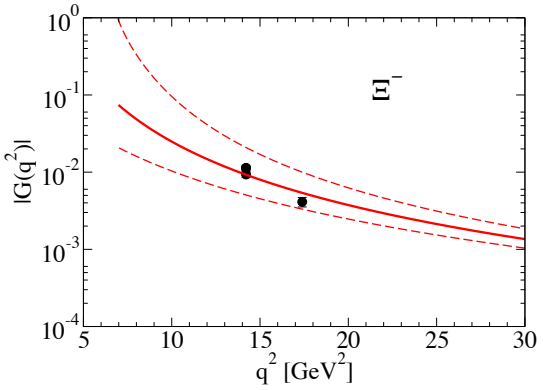


$$G_M(q^2) \simeq G_M^{\rm SL}(-q^2),$$
$$G_E(q^2) \simeq G_E^{\rm SL}(-q^2).$$

Uncertainty bar:

Full line: $G(q^2) = G(2M^2 - q^2)$

Dashed lines: $G(q^2) = G(4M^2 - q^2)$

$G(q^2) = G(-q^2)$

Guidance for determination of onset of ”reflection” symmetry

**G. Ramalho and M.T.P. Phys.Rev.D 101 (2020) 1, 014014, (2020)**

# $\gamma N \rightarrow \Delta$

## Connection to Lattice QCD

To control model dependence:

CST model and LQCD data are made **compatible.**

G. Ramalho and M. T. Peña, Phys. Rev. D 80, 013008 (2009)

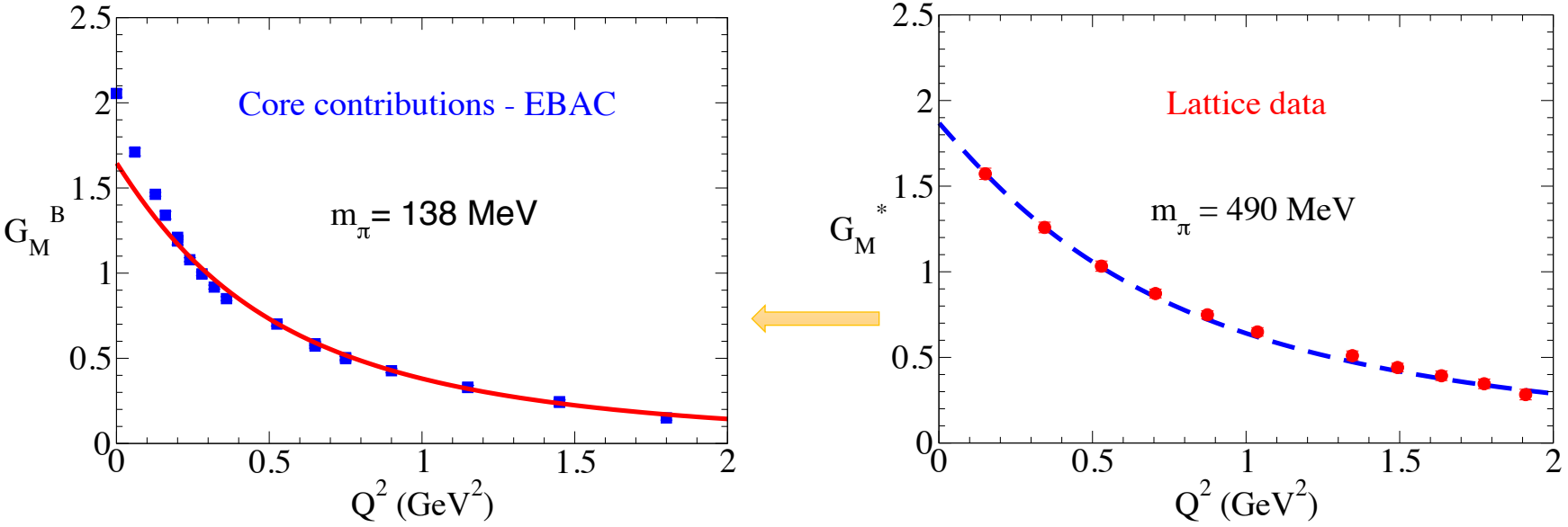


Model (no pion cloud) valid for lattice pion mass regime.

No refit of wave function scale parameters for the physical pion mass limit.

# E.M. Current and TFF near the photon point

Pseudo Threshold PT $\quad Q_0^2 = -(M_R - M_N)^2 \;\; ; |\vec{Q}| = 0$

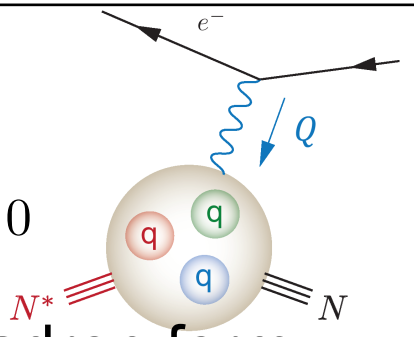


An accident of the definition of the Jones and Scadron form factors:

$$G_E(PT) = \frac{M_R - M}{2M_R} G_C(PT)$$

A form of the "Siegert condition"!
This is implied by orthogonality of states.
If data analysis proceed through helicity amplitudes
this behavior may be missed.

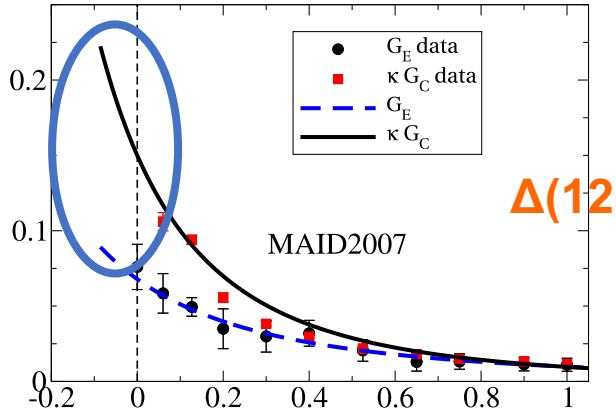


G.Ramalho Phys. Lett. B 759 (2016) 126

# $G_E$ and $G_C$

$\gamma N \rightarrow \Delta$

Large $N_C$ limit and SU(6) quark models:

- Suggest that pion cloud effects for $G_E$ and $G_C$ generate deviations from the Siegert condition of the order $\mathcal{O}(1/N_c^2)$ and do not agree to data at low $Q^2$.

Corrected parametrization with deviations $\mathcal{O}(1/N_c^4)$ generated agreement with 2017 JLAB data

G. Ramalho Phys. Rev. D94,114001,(2016)

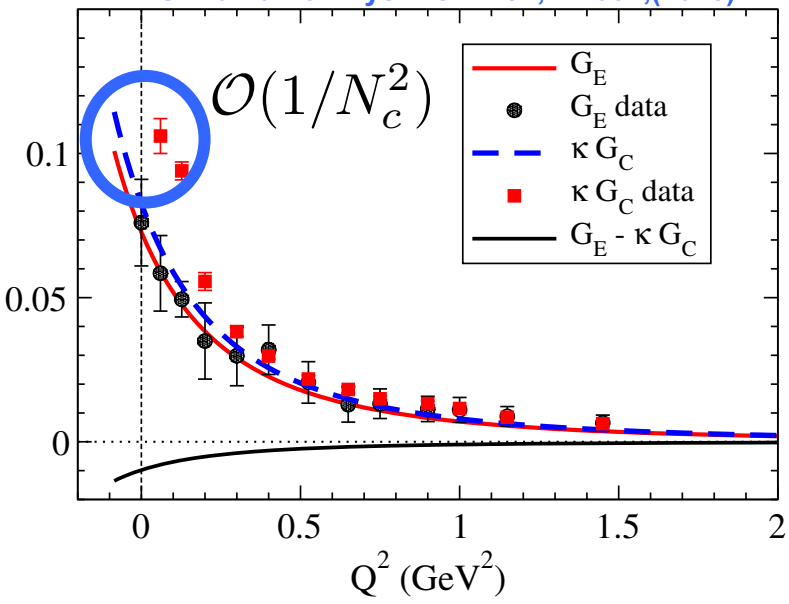


G. Ramalho Eur.Phys.J. A54 (2018) no.5, 75

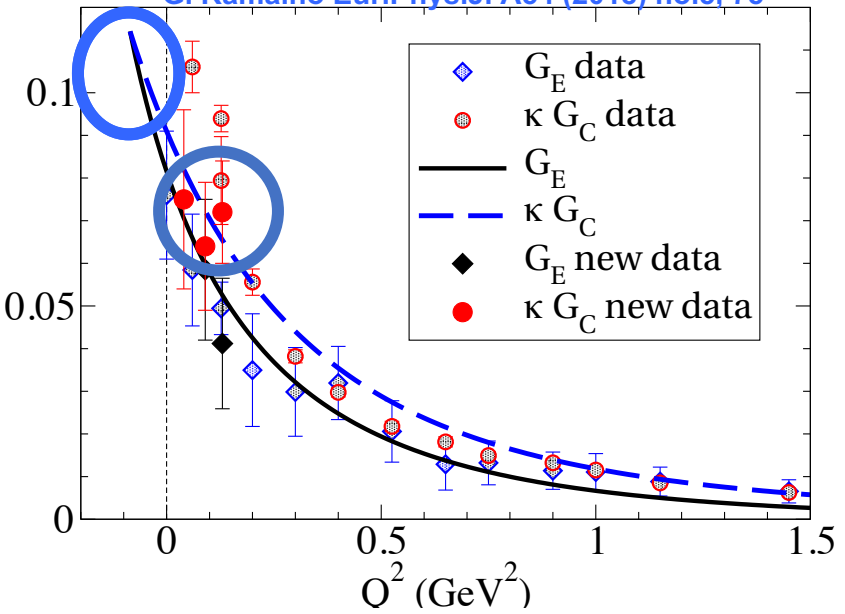

# Extension to Timelike

$$\gamma N \rightarrow \Delta$$

- Extension to higher W shows effect of the rho mass pole
- In that pole region small bare quark contribution (thin lines)

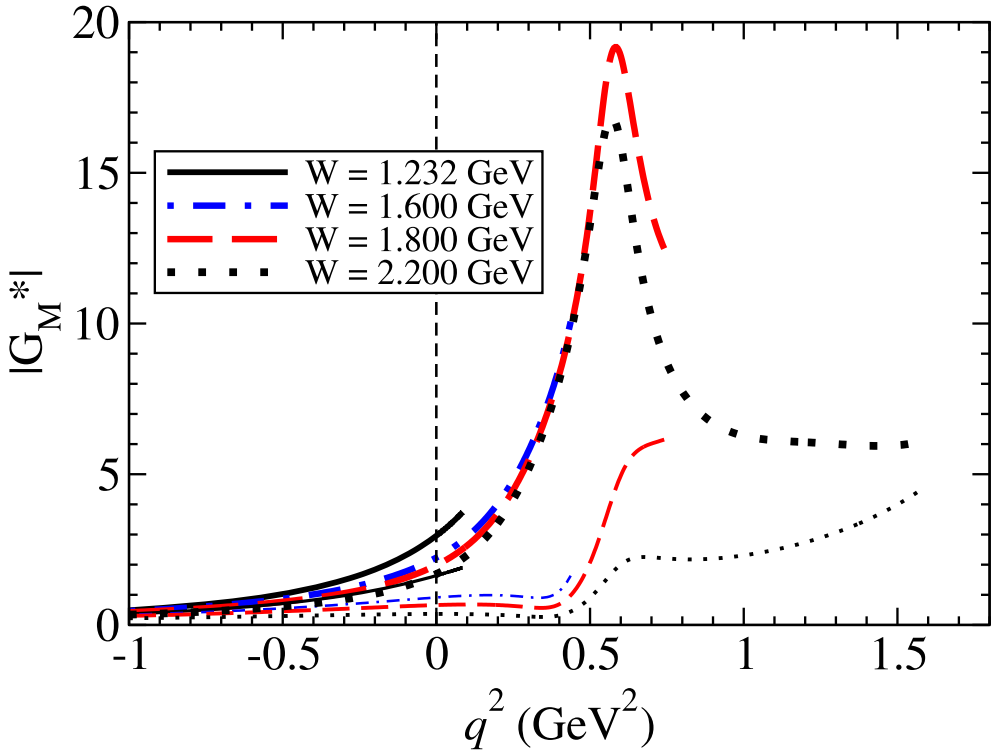

# Crossing the boundaries

N*(1535) Dalitz decay

$$\Gamma_{\gamma^* N}(q,W) = \frac{\alpha}{2W^3}\sqrt{y_+ y_-}\, y_+ B \|G_T(q^2,W)|^2,$$

$$|G_T(q^2,W)|^2 = |G_E(q^2,W)|^2 + \frac{q^2}{2W^2}|G_C(q^2,W)|^2$$

$$\frac{d\Gamma_{e^+e^-N}}{dq}(q,W) = \frac{2\alpha}{3\pi q^3}(2\mu^2+q^2)\sqrt{1-\frac{4\mu^2}{q^2}}\,\Gamma_{\gamma^* N}(q,W),$$

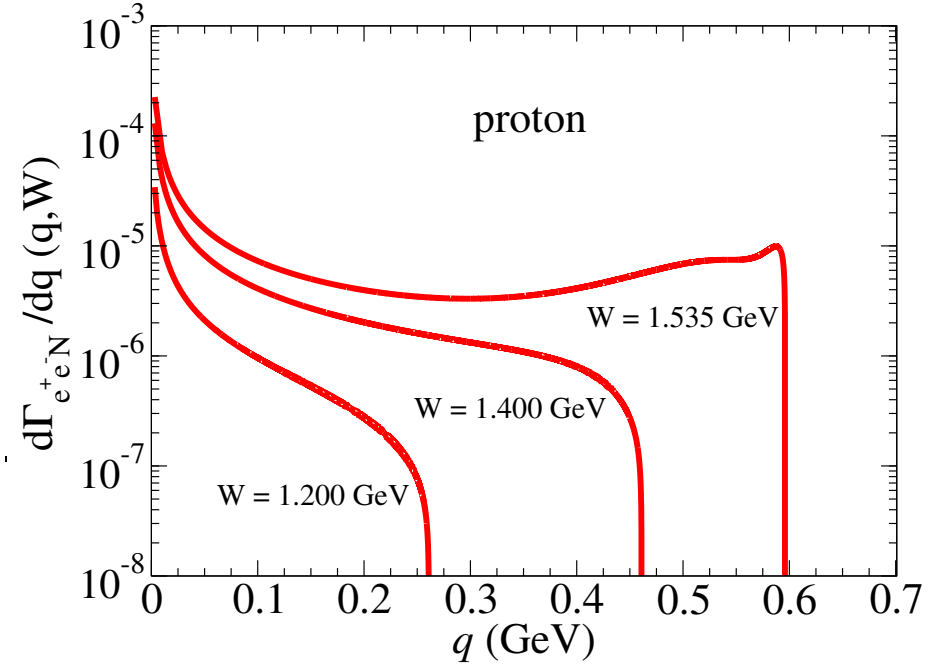


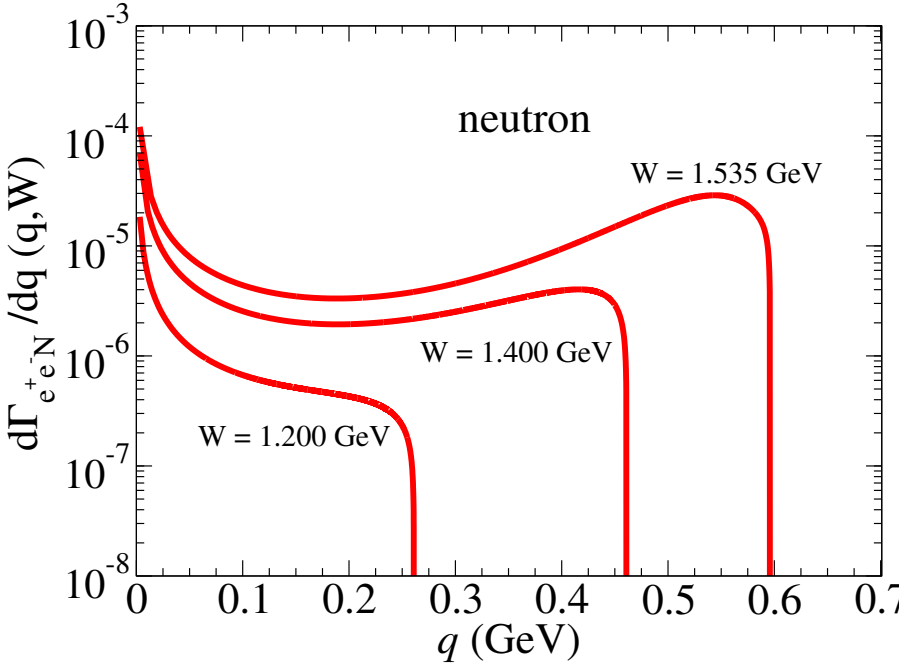

# Predictive power:

D13(J=3/2-) **S11**(J=1/2-) (I=1/2) are part of a large supermultiplet (SU(6) spin-flavor with O(3) symmetry)

S. Capstick and W. Roberts, Prog. Part. Nucl. Phys. 45, S241 (2000);
V. D. Burkert et al. Phys. Rev. C 67, 035204 (2003).

**Input:** $N(1520), N(1535)$; **Output:** $N(1650), N(1700), \Delta(1620), \Delta(1700)$

D13 **S11** **S11** D13 **S31** D33

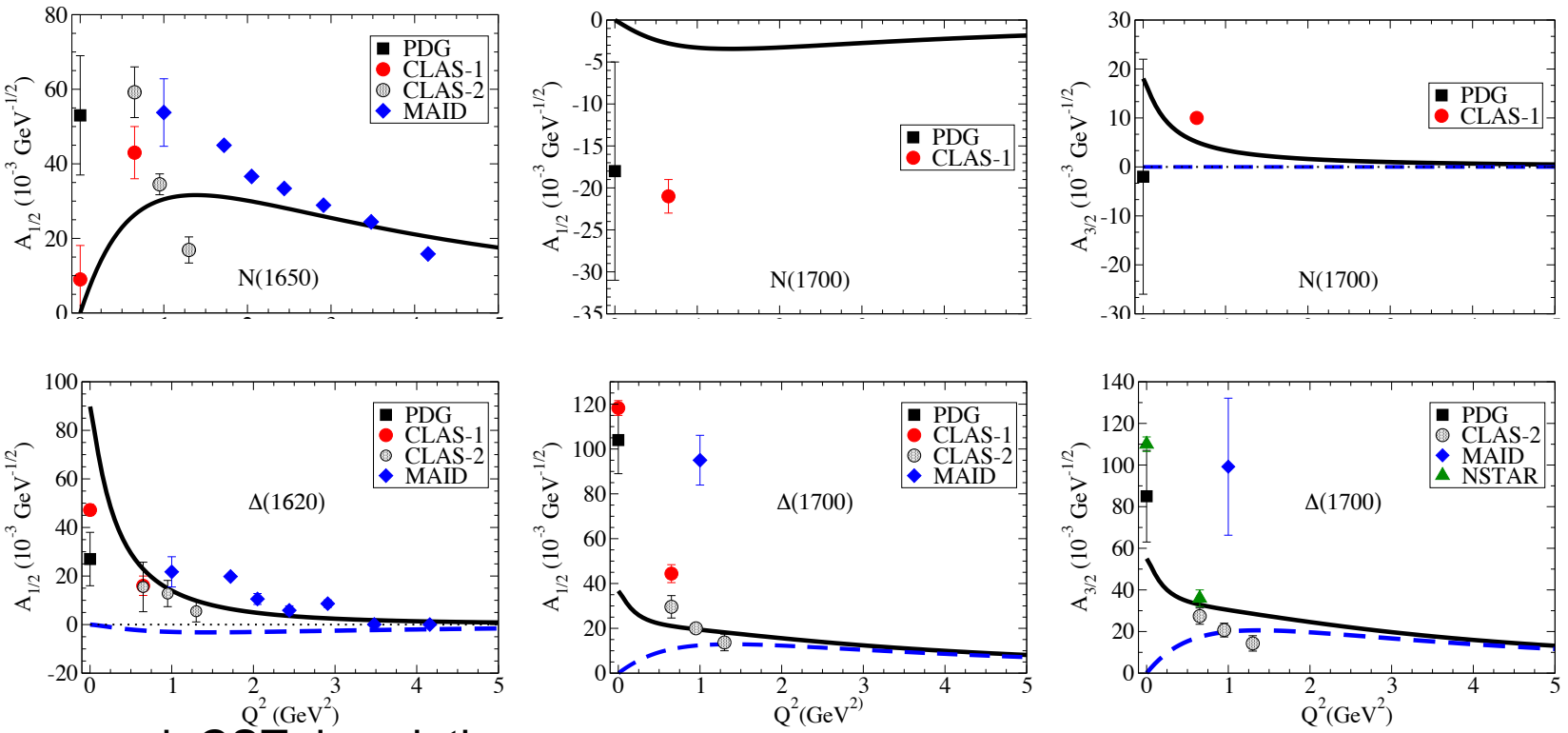


Bare quark CST description expected to work well in high $Q^2$ region!

G. Ramalho , PRD 90, 033010 (2014)